

Accepted Manuscript

Design, synthesis and biological evaluation of novel isoindolinone derivatives as potent histone deacetylase inhibitors

Xin Chen, Shuang Zhao, Hongmei Li, Xin Wang, Aixin Geng, Hao Cui, Tao Lu, Yadong Chen, Yong Zhu



PII: S0223-5234(19)30146-1

DOI: <https://doi.org/10.1016/j.ejmech.2019.02.032>

Reference: EJMECH 11124

To appear in: *European Journal of Medicinal Chemistry*

Received Date: 5 November 2018

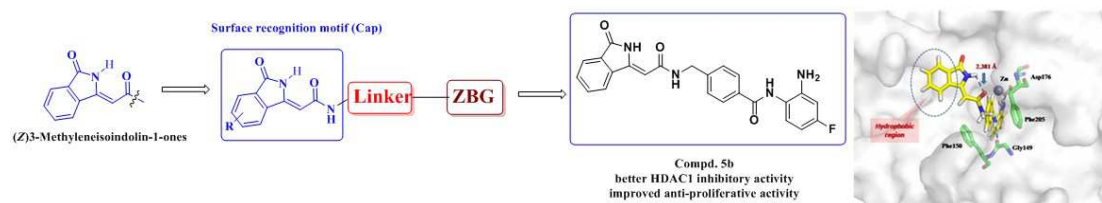
Revised Date: 10 February 2019

Accepted Date: 10 February 2019

Please cite this article as: X. Chen, S. Zhao, H. Li, X. Wang, A. Geng, H. Cui, T. Lu, Y. Chen, Y. Zhu, Design, synthesis and biological evaluation of novel isoindolinone derivatives as potent histone deacetylase inhibitors, *European Journal of Medicinal Chemistry* (2019), doi: <https://doi.org/10.1016/j.ejmech.2019.02.032>.

This is a PDF file of an unedited manuscript that has been accepted for publication. As a service to our customers we are providing this early version of the manuscript. The manuscript will undergo copyediting, typesetting, and review of the resulting proof before it is published in its final form. Please note that during the production process errors may be discovered which could affect the content, and all legal disclaimers that apply to the journal pertain.

GRAPHICAL ABSTRACT



Design, Synthesis and Biological Evaluation of Novel Isoindolinone Derivatives as Potent Histone Deacetylase Inhibitors

Xin Chen^a, Shuang Zhao^b, Hongmei Li^b, Xin Wang^c, Aixin Geng^b, Hao Cui^b, Tao Lu^{b, d}, Yadong Chen^{b, *}, Yong Zhu^{b, *}

^aShaanxi Key Laboratory of Natural Products & Chemical Biology, College of Chemistry & Pharmacy, Northwest A&F University, Yangling 712100, P. R. China

^bSchool of Science, China Pharmaceutical University, Nanjing, 210009, P. R. China

^cSchool of Pharmacy, China Pharmaceutical University, Nanjing 210009, P. R. China

^dState Key Laboratory of Natural Medicines, China Pharmaceutical University, 24 Tongjiaxiang, Nanjing, 210009, P. R. China

Corresponding Author

*Yadong Chen

E-mail: ydchen@cpu.edu.cn; Fax: +86-25-86185170

*Yong Zhu

E-mail: zhuyong@cpu.edu.cn; Fax: +86-25-86185182

Notes

The author declare no competing interest.

Abstract

Histone deacetylases (HDACs) as appealing targets for the treatment of many diseases has been studied extensively and its use in cancer care is the most important. Here, we developed a series of novel derivatives containing isoindolinone skeleton. Twelve compounds demonstrated nanomolar IC₅₀ values against HDAC1, and the best compounds were **5a** (65.6 nM), **5b** (65.1 nM) and **13a** (57.9 nM). In vitro, **5a** and **5b** also showed potent antiproliferative activities against several cancer cell lines, in particular **5b**, which behaved better than approved drug chidamide. Moreover, enzyme inhibition and western blot assay established **5b** to be a selective inhibitor for HDAC1-3. Molecular docking was performed to rationalize the high potency of isoindolinones. Additionally, **5b** had more appropriate drug metabolism in human liver microsome (HLM) compared with chidamide and moderate pharmacokinetics properties. These results indicated that **5b** was worthy of further biological studies.

Keywords

HDAC inhibitor; Antiproliferation; Isoindolinone; Synthesis ; Structural optimization

1. Introduction

Histone lysine acetylation is an epigenetic marker associated with gene transcriptional activation and repression[1]. Histone deacetylases (HDACs), which remove acetyl groups from lysine residues in histones or non-histone substrates, are overexpressed in many kinds of cancers. Inhibition of HDACs gives rise to anticarcinogenic effects through several different mechanisms including reduced cell motility/migration, invasion, induction of apoptosis, angiogenesis, and blocking of DNA repair. As a result, HDACs have emerged as an attractive target for the tumor therapy[2-5]. The human HDACs family containing 18 isoforms is divided into class I (HDACs 1, 2, 3 and 8), class IIa (HDACs 4, 5, 7 and 9), class IIb (HDACs 6 and 10), class III (named sirtuins 1-7) and class IV (HDAC 11). The classical HDACs refer to class I, II and IV isoforms which require zinc ion as a cofactor for deacetylating activity, while that of class III isoforms is nicotinamide adenine dinucleotide[6-8]. Each HDAC isotype has different biological function. Specifically, class I HDACs are widespread across all tissues and

play key role in epigenetic processes [9-12]. Moreover, they are highly expressed in a number of cancers and sustain malignant growth, enabling tumor cells susceptible to HDAC inhibitors (HDACis).

To date, numerous HDACis have been exploited, several of which have been approved for cancer treatment. Nonselective hydroxamic acid inhibitors, such as vorinostat (SAHA)[13], belinostat (PXD-101)[14], panobinostat (LBH-589)[15] and natural romidepsin (FK228)[16] have gained U.S. Food and Drug Administration approvals for the treatment of cutaneous T-cell lymphoma, peripheral T-cell lymphoma and multiple myeloma. Chidamide, a benzamide inhibitor which was reported to be a class I selective HDACi[17-18], was approved for treating recurrent and refractory peripheral T-cell lymphoma by the China Food and Drug Administration in 2015 (**Fig. 1**).

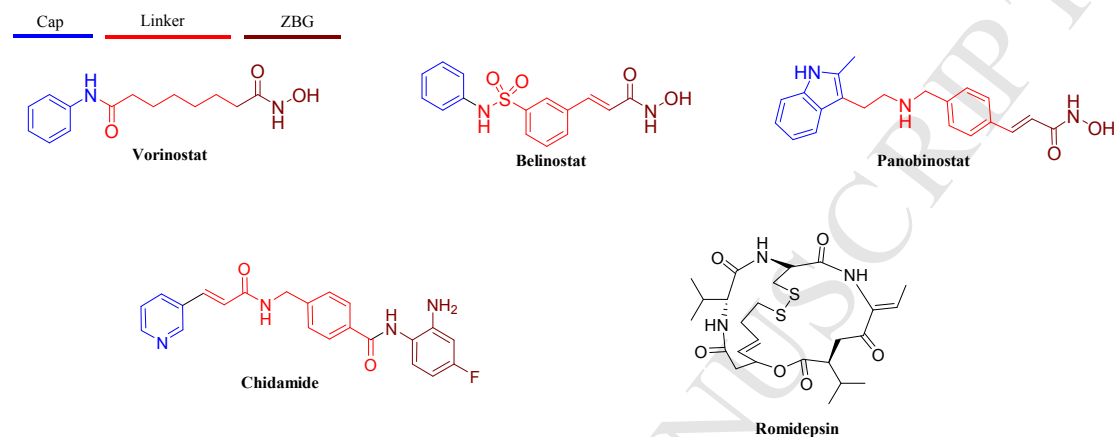


Fig.1. Approved HDACs inhibitors

Generally, HDAC inhibitors have common structural characteristics: cap, linker and zinc binding group (ZBG) [19]. Cap moiety matches the rim region of the protein pocket, greatly influencing inhibitory potency and isoforms selectivity. It usually contains large aromatic group such as aryl or heteroaryl[20-21]. Macrocyclic structures as cap moiety was also reported[22]. Linker segment embeds into the native channel and makes the ZBG in a proper position to chelate with the catalytic zinc ion below. Unlike the well-established linker and ZBG group, modification of cap moiety generates a lot of novel potent inhibitors. Among these, a large and rigid aromatic capping group is considered to be a key portion for favoring the interaction between the molecular and HDACs. Moreover, inhibitor bearing a rigid skeleton usually exhibits a favorable metabolism profile[23-24].

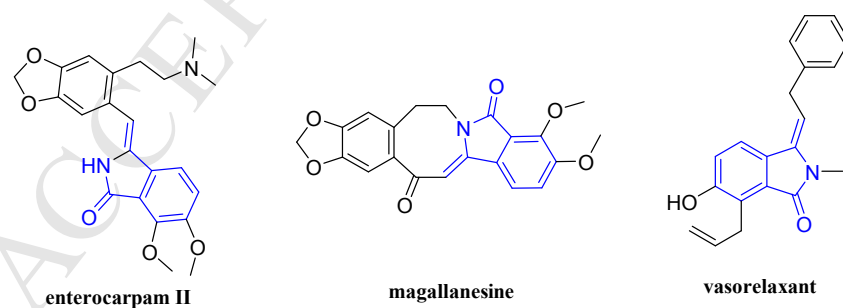


Fig. 2 Known 3-methyleneisoindolin-1-one-based bioactive compounds

Isoindolinones are important scaffolds in medicinal chemistry and organic chemistry for their prevalence in many natural and synthetic bioactive molecules. In particular, 3-methyleneisoindolin-1-ones have been recognized as core components in natural products such as enterocarpam II, the secophthalide-isoquinoline ene-lactam fumaridine[25], magallanesine, an isoindolobenzazocine derived from the South-American plant *Berberis darwinii*[26]. 3-Methyleneisoindolin-1-ones with vasorelaxant activity were also reported[27] (**Fig. 2**). These

results prompted us to identify novel potential HDAC inhibitors based on the inflexible isoindolinone skeleton. In the previous study, we described an efficient stereoselective synthesis of (*Z*) 3-methyleneisoindolin-1-ones via base-catalyzed intermolecular reaction[28]. With this result in hand, we synthesized a series of novel HDACis bearing rigid (*Z*) 3-methyleneisoindolin-1-one as capping group in combination with various linkers and ZBGs (**Fig. 3**). Here, we report the design, synthesis, structure–activity relationship (SAR) and metabolism researches of this new class of HDACis.

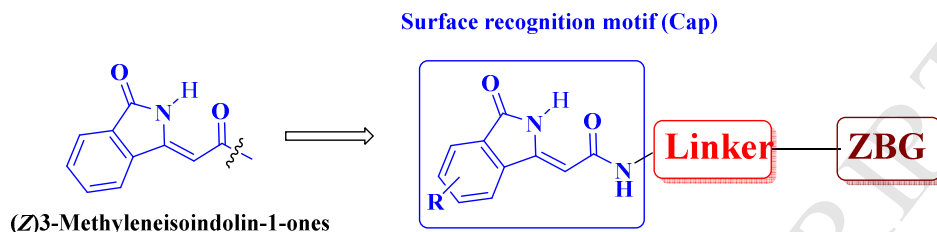
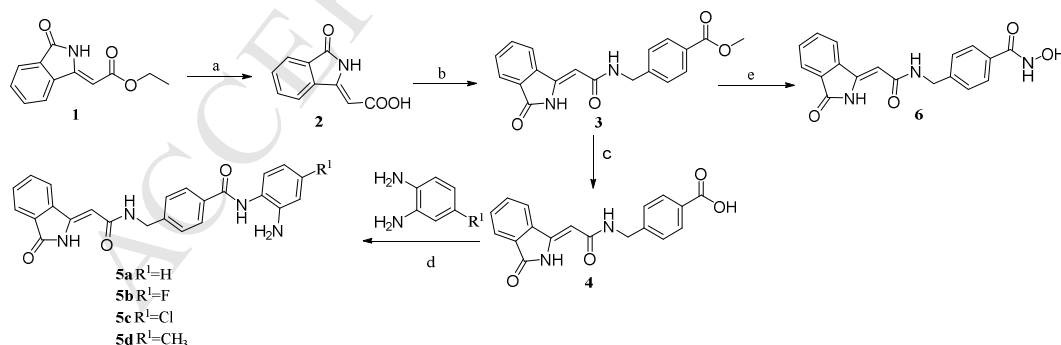


Fig. 3. Design of our isoindolinone-based HDACis

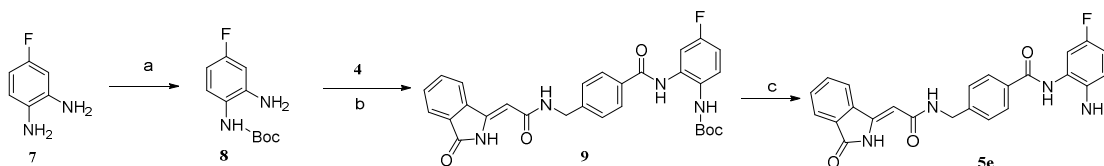
2. Results and discussion

2.1 Chemistry

To evaluate the effect on enzymatic activity of the linker between ZBG and the isoindolinone capping group, compounds **5a-e**, **6** with phenyl linkers and **12a-d**, **13a-b** with chain linkers were synthesized. Among these, 2-aminobenzamides and hydroxamic acid moieties were chosen as ZBG respectively. Compounds **5a-d** were synthesized as shown in **Scheme 1**. (*Z*) 3-methyleneisoindolin-1-one derivative **1** was synthesized as the procedure which we previously reported[21]. Hydrolyzation of **1** with lithium hydroxide (LiOH) in methanol (MeOH) afforded intermediate **2**. Amidation of compound **2** with methyl 4-(aminomethyl)benzoate hydrochloride using 2-(7-Azabenzotriazol-1-yl)-*N,N,N',N'*-tetramethyluronium hexafluorophosphate (HATU) gave intermediate **3**. Subsequent hydrolysis of **3** yielded compound **4**. Coupling of **4** with benzene-1, 2-diamine and various substituted benzene-1, 2-diamine gave target compounds **5a-d**. Under basic conditions, the methyl ester group of **3** was directly converted to the corresponding hydroxamic acid **6** by hydroxylamine (NH₂OH). Compound **5e** was synthesized as shown in **Scheme 2**. The synthesis of intermediate **8** was performed starting from 4-fluorobenzene-1, 2-diamine (**7**), the amino was selectively protected in a (Boc)₂O/KHCO₃ system. Then **8** reacted with **2** by HATU-mediated amide formation to afford **9**. The Boc protecting group was subsequently removed in the presence of trifluoroacetic acid (TFA), which generated the desired compound **5e**.

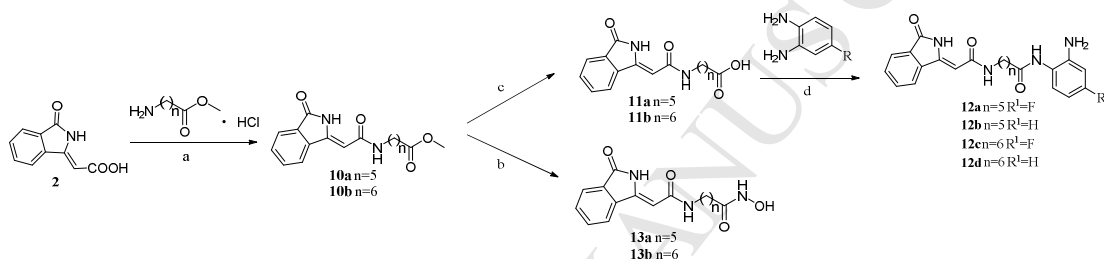


Scheme 1. Synthesis of compounds **5a-d** and **6**. Reagents and conditions: (a) LiOH, MeOH, 50 °C, 2 h; (b) HATU, *N,N*-diisopropylethylamine (DIPEA), *N,N*-dimethylformamide (DMF), Methyl 4-(aminomethyl)benzoate hydrochloride, r.t., 6 h; (c) LiOH, MeOH, 60 °C, 2 h; (d) HATU, DIPEA, DMF, r.t., 6 h; and (e) NH₂OH, KOH, MeOH, r.t., overnight.



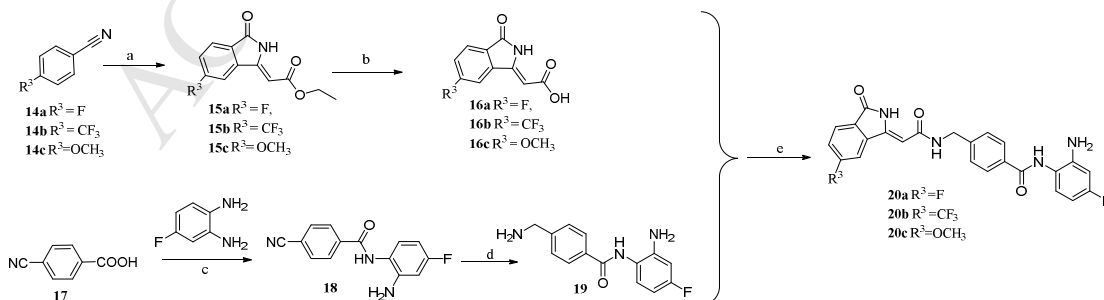
Scheme 2. Synthesis of compound **5e**. Reagents and conditions: (a) (Boc)₂O, KHCO₃, CH₃CN, 0 °C ~30 °C, 4 h; (b) HATU, DIPEA, andrydrous DMF, r.t., 10 h; and (c) DCM/TFA (v:v = 1:1), 0 °C, 10 h.

Then we changed phenyl linker with common chain linkers which had different lengths. A series of isoindolinone analogues (**12a-d**, **13a-b**) were synthesized as shown in **Scheme 3**. Amidation of **2** with commercial methyl 6-aminohexanoate or methyl 7-aminohexanoate gave intermediates **10a** or **10b**, respectively. The intermediates **10a-b** were then converted to hydroxamic acids **13a-b** in good yields under conditions similar to those shown in **Scheme 1**. The coupling of different benzene-1, 2-diamines with the hydrolysates of compounds **10a-b** generated the target compounds **12a-d**.

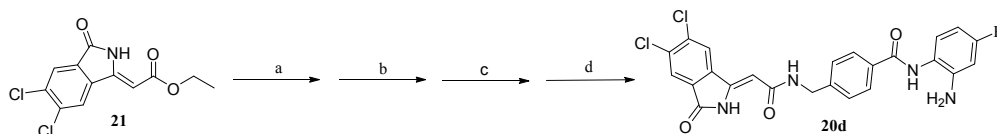


Scheme 3. Synthesis of compounds **12a-d** and **13a-b**. Reagents and conditions: (a) HATU, DIPEA, DMF, 6-aminohexanoate or methyl 7-aminohexanoate hydrochloride, r.t., 6 h; (b) NH₂OH, KOH, MeOH, r.t., overnight; (c) LiOH, MeOH, 50 °C, 2 h; and (d) HATU, DIPEA, DMF, r.t., 6 h;

To explore the structure and activity relationship of cap motif, different substituents were introduced on the phenyl of isoindolinone. Compounds **20a-c** were synthesized as shown in **Scheme 4**. Cyclizations of substituted benzonitriles **14a-c** and ethyl acrylate in the presence of RuCl₂ as catalyst gave the key isoindolinones **15a-c**[29], which then were hydrolyzed with lithium hydroxide to give **16a-c**. Compound **19** was prepared through two steps: the first synthetic step involved in the amidation of 4-cyanobenzoic acid **17** with 4-fluorobenzene-1,2-diamine to afford **18**, and then **18** was reduced by hydrogen in the presence of Pd/C. Target compounds **20a-c** were obtained by coupling of intermediates **16a-c** with **19** in the presence of HATU. In addition, dichloro-substituted isoindolinone derivative **20d** was synthesized beginning with the (Z)-ethyl 2-(5, 6-dichloro-3-oxoisoindolin-1-ylidene)acetate (**21**, **Scheme 5**) under conditions similar to those shown in **Scheme 1**.

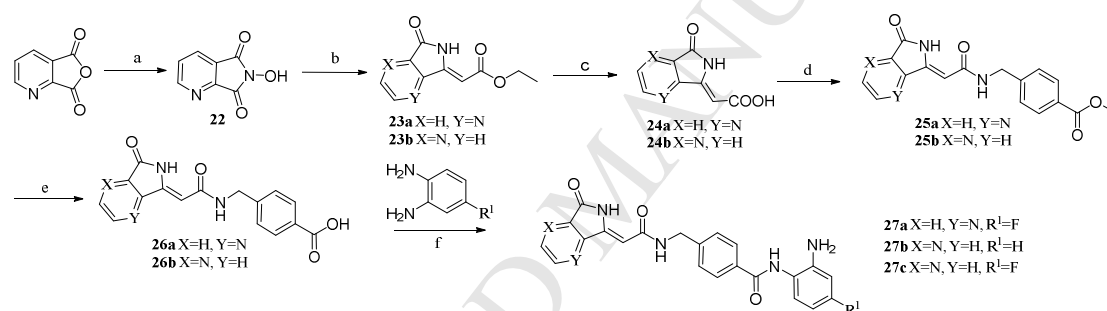


Scheme 4. Synthesis of compounds **20a-c**. Reagents and conditions: (a) Dichloro(*p*-cymene)ruthenium(II) dimer, AgSbF₆, Cu(OAc)₂ H₂O, ethyl acrylate, AcOH, 120 °C, 24 h; (b) LiOH, MeOH, 60 °C, 6 h; (c) HATU, DIPEA, DMF, r.t., 12 h; (d) H₂, Pd/C, MeOH, r.t., 4 h; and (e) HATU, DIPEA, DMF, r.t., 6 h.



Scheme 5. Synthesis of compound **20d**. Reagents and conditions: (a) LiOH, MeOH, 60 °C, 2 h; (b) HATU, DIPEA, DMF, Methyl 4-(aminomethyl)benzoate hydrochloride, r.t., 6 h; (c) LiOH, MeOH, 50 °C, 2 h; and (d) 4-fluorobenzene-1,2-diamine, HATU, DIPEA, DMF, r.t., 6 h;

Considering that the surface of the active pocket where the capping group binds is adjacent to the solvent accessible region, increasing the polarity of cap moiety was a logical choice. Hence, we introduced nitrogen atom to the phenyl of isoindolinone scaffold yielding two novel azaisoindolinone scaffolds **23a** and **23b**. Up to now, there is no literatures have revealed the structures and synthesis route of **23a** and **23b**, thus we tried to obtain them follow the same procedure as in isoindolinones. 6-hydroxy-5*H*-pyrrolo[3,4-*b*]pyridine-5,7(6*H*)-dione (**22**) was obtained by ammonolysis reaction of furo[3,4-*b*]pyridine-5,7-dione with hydroxylamine hydrochloride using acetic acid as solvent. As we anticipated, reaction of (**22**) with ethyl propionate generated cyclization azaisoindolinones **23a** and **23b** simultaneously in equal yields, and the structures of which were further characterized by X-ray crystallography (see supporting information). With the key intermediates **23a** and **23b** in hand, target compounds **27a-c** were synthesized (**Scheme 6**) under conditions similar to those shown in **Scheme 1**.



Scheme 6. Synthesis of compounds **27a-c**. Reagents and conditions: (a) hydroxylamine hydrochloride, AcOH, 119 °C, 4 h; (b) tributylphosphine (Bu₃P), ethyl propionate, anhydrous DMF, 150 °C, 2 h; (c) LiOH, MeOH, 50 °C, 2 h; (d) HATU, DIPEA, DMF, Methyl 4-(aminomethyl)benzoate hydrochloride, r.t., 6 h; (e) LiOH, MeOH, 50 °C, 2 h; and (f) substituted benzene-1,2-diamine, HATU, DIPEA, DMF, r.t., 6 h;

2.2 HDAC inhibition and SAR study of target compounds

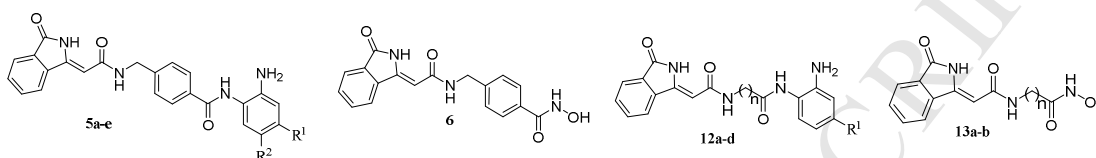
We tested all acquired compounds for inhibitory ability against HDAC1, using chidamide and SAHA as references. We selected the HDAC1 enzyme because it was widely involved in transcriptional repression and was intimately linked to the tumors. Compounds **5a-e**, **6**, **12a-d** and **13a-b** were synthesized to evaluate the influence of the modifications of linker and ZBG on HDAC1 activity. As shown in **Table 1**, the inhibition rates (IRs) against HDAC1 of most tested compounds were above 70% at 50 μM concentration except **6** and **13b**. IC₅₀ results illustrated that the benzamide compounds **5a**, **5b**, and **5e**, with IC₅₀ values of 65.6, 65.1 and 70.3 nM, exhibited better activities than chidamide (IC₅₀ = 296 nM). Hydroxamic acid analogue **13a** also showed a potent HDAC1 inhibition with IC₅₀ value of 57.9 nM, although this was obviously weaker than SAHA (IC₅₀ = 4 nM).

When we chose 2-aminobenzamide moiety as ZBG, the HDAC1 inhibitory activities were markedly influenced by different substituents on the phenyl of ZBG group. Fluorine (F) atom was similar in size and bulk with hydrogen (H) atom, therefore introducing F substituent on the *para*-position of the amide (R¹ position) had marginal influence on the HDAC1 potency, i.e. **5b** vs **5a**. However, replacement of F with larger chlorine (**5c**, IC₅₀ = 466 nM) or methyl (**5d**, IC₅₀ = 5.72 μM) substituents decreased the HDAC1 potency substantially which might

be attributed to the resulting hindrance at R¹ position. While changing the F substituent from R¹ to R² position, compound **5e** still exhibited a comparable HDAC1 activity. Compounds **5a**, **5b** with phenyl as linker showed better HDAC1 inhibitory activity than compounds **12a-d** with aliphatic chain as linker whose IC₅₀ values distributed between 320 nM and 6.42 μM. When we chose hydroxamic acid as ZBG, compound **6** with phenyl as linker only had a HDAC1 IR of 49.91% at 50 μM concentration. Compound **13a** with a five carbon length chain as linker (n = 5) displayed an excellent activity (IC₅₀ = 57.9 nM), whereas increasing the length of the aliphatic chain to six carbon as in **13b** resulted in a lost of HDAC1 inhibition. The inappropriate linker lengths of hydroxamic acids **6** (IR = 49.91%) and **13b** (IR = 15.49%) might be responsible for the decrease of HDAC1 activity.

Table 1

The HDAC1 inhibitory activity of compounds **5a-e**, **6**, **12a-d** and **13a-b**.



| Cpd. | R ¹ | R ² | HDAC1 | | Cpd. | n | R ¹ | HDAC1 | |
|-------------|-----------------|----------------|--------------------------|------------------------------------|------------------|---|----------------|--------------------------|------------------------------------|
| | | | IR% ^a (50 μM) | IC ₅₀ ^b (μM) | | | | IR% ^a (50 μM) | IC ₅₀ ^b (μM) |
| 5a | H | H | 99.28 | 0.0656±0.0092 | 12a | 5 | F | 75.60 | 6.4200±0.3253 |
| 5b | F | H | 99.31 | 0.0651±0.0073 | 12b | 5 | H | 89.96 | 0.8720±0.0037 |
| 5c | Cl | H | 90.63 | 0.4660±0.0524 | 12c | 6 | F | 81.57 | 1.6000±0.1573 |
| 5d | CH ₃ | H | 81.60 | 5.7200±0.8476 | 12d | 6 | H | 93.98 | 0.3200±0.0299 |
| 5e | H | F | 99.23 | 0.0703±0.0051 | 13a | 5 | / | 97.30 | 0.0579±0.0061 |
| 6 | / | / | 49.91 | - ^c | 13b | 6 | / | 15.49 | - |
| SAHA | | | 99.87 | 0.0040±0.0007 | Chidamide | | | 90.92 | 0.296±0.0417 |
| TSA | | | 99.36 | 0.0125±0.0012 | | | | | |

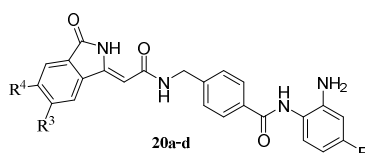
^aIR%: Enzymatic inhibition rate of HDAC1 was tested at 50 μM. ^bIC₅₀ values for enzymatic inhibition of HDAC1. ^c- : not tested. We ran experiments in duplicate. Assays were performed by Reaction Biology Corporation (Malvern, PA, USA).

The preliminary enzymatic results outlined in **Table 1** demonstrated that the strategy of introducing isoindolinone as the capping group was rational and feasible. In consideration of chemical instability, potential toxicity^[30] of hydroxamic acid HDACis, and lower potency against HDAC1 of **13a** compared with SAHA, further modification on isoindolinone was performed based on benzamide analogue **5b** with 2-aminobenzamide moiety as ZBG and phenyl as linker. As shown in **Table 2**, the introduction of different substituents on capping group had a detrimental impact on HDAC1 activity. Electron withdrawing groups like F (**20a**) or large trifluoromethyl (**20b**) at R³ position led to a 3-fold and 8-fold decrease on potency than that of **5b**, with IC₅₀ values of 167 nM and 491 nM, respectively. Dichloro-substituted (R³ and R⁴ positions) analogue **20d**, were also over seven times less potent compared to **5b**, with an IC₅₀ value of 489 nM. Moreover, a slightly reduced enzymatic activity was also observed for compound **20c** (IC₅₀ = 96.8 nM) with an electron donor methoxy group at R³ position. The general trend established was that an electron donor substituent on isoindolinone was more favorable for HDAC1 activity than electron withdrawing group.

When the phenyl of isoindolinone was replaced with pyridine, we observed a sharp fall on HDAC1 inhibitory potency for compound **27a** and **27c** compared with **5b**. Azaisoindolinone **27b** without a fluoro substituent on ZBG also had a nearly 12-fold decrease in comparison with **5a**. These results indicated that a more hydrophobic structure might be suitable for binding with the surface area of HDAC1.

Table 2

HDAC1 inhibitory activities of compounds **20a-d** and **27a-c**.



| Cpd. | R ³ | R ⁴ | HDAC1 | |
|------------------|------------------|----------------|--------------------------|------------------------------------|
| | | | IR% ^a (50 μM) | IC ₅₀ ^b (μM) |
| 20a | F | H | 94.43 | 0.1670±0.0189 |
| 20b | CF ₃ | H | 93.49 | 0.4910±0.0713 |
| 20c | OCH ₃ | H | 94.26 | 0.0968±0.0117 |
| 20d | Cl | Cl | 92.38 | 0.4890±0.0614 |
| 27a | | | 62.93 | NA ^c |
| 27b | | | 88.53 | 0.7580±0.1094 |
| 27c | | | 50.38 | 8.3600±0.8365 |
| Chidamide | | | 90.9 | 0.2960±0.0433 |

^aIR%: Enzymatic inhibition rate of HDAC1 was tested at 50 μM. ^bIC₅₀ values for enzymatic inhibition of HDAC1. ^cNA: no inhibition activity. We ran experiments in duplicate. Assays were performed by Reaction Biology Corporation (Malvern, PA, USA).

To investigate the selectivity of benzamide isoindolinones versus other HDAC isoforms, the representative **5b** was tested against all of the 11 class I, II and IV HDACs with chidamide as reference compound. As described in **Table 3**, **5b** preferentially inhibited HDAC1-3 (IC₅₀ values of 65.1, 75 and 112 nM, respectively) and almost lost activity against class II HDACs, indicating a similar selectivity profile to that of chidamide. Moreover, a 17-fold and 10-fold selectivity toward HDAC8 and HDAC11 versus HDAC1 were also observed for **5b**. These data displayed that **5b** was a potent class I selective HDACs inhibitor.

Table 3

Complete Characterization of **5b** at all 11 class I, II, and IV HDACs (IC₅₀^a, μM).

| Zn ²⁺ -dependent HDAC isoforms | | 5b | Chidamide |
|---|-------------|-----------------|------------------|
| Class I | HDAC1 | 0.0651±0.0049 | 0.2960±0.0117 |
| | HDAC2 | 0.0750±0.0009 | 0.4500±0.0216 |
| | HDAC3 | 0.1120±0.0082 | 0.2650±0.0005 |
| | HDAC8 | 1.0800±0.0305 | 0.8330±0.0073 |
| Class IIa | HDAC4/5/7/9 | NA ^b | NA |
| Class IIb | HDAC6 | NA | NA |
| | HDAC10 | 0.9500±0.0913 | 0.2350±0.0227 |
| Class IV | HDAC11 | 0.6320±0.0315 | 0.7600±0.0771 |

^aIC₅₀ values for enzymatic inhibition of HDACs. ^bNA: no inhibition activity. We ran experiments in duplicate. Assays were performed by Reaction Biology Corporation (Malvern, PA, USA).

2.3 In vitro antiproliferative activity

On the basis of the enzymatic results above, the most promising compounds **5a** and **5b** was determined to evaluate antiproliferative activities of isoindolinones against human leukemia cell lines HL-60 and K562, colon cancer cell line HCT116 and breast cancer cell line MCF-7 (the results are summarized in **Table 4**). As we expected, both **5a** and **5b** exhibited excellent inhibitory activities against HL-60 and K562 cell lines with IC_{50} values ranging from 193 to 450 nM. In addition, nanomolar antiproliferative activities against solid tumor cell line HCT116 were also observed. Notably, **5a**, **5b** and chidamide were less potent in inducing MCF-7 cell death with IC_{50} values in double-digit micromolar range. Compound **5b**, with a lipophilic F substituent on the terminal phenyl, showed better antiproliferative activity than **5a** despite of their equipotent HDAC1 inhibition. This could be attributed to the increased lipophilicity which made **5b** penetrate cell membrane more easily. Compared with chidamide, **5b** displayed overall superior antiproliferative activities including HL-60 (5-fold), K562 (4-fold), HCT116 (2.5-fold) and MCF-7 (2-fold).

Table 4

Antiproliferative activity of **5a**, **5b** and reference inhibitor chidamide against HL-60, K562, HCT116 and MCF-7 cell lines

| Compound | IC_{50} , μ M | | | |
|-----------|---------------------|-------------------|-------------------|--------------------|
| | HL-60 | K562 | HCT116 | MCF-7 |
| 5a | 0.450 \pm 0.067 | 0.286 \pm 0.039 | 0.483 \pm 0.071 | 20.080 \pm 1.641 |
| 5b | 0.373 \pm 0.046 | 0.193 \pm 0.020 | 0.432 \pm 0.055 | 14.560 \pm 2.133 |
| Chidamide | 1.970 \pm 0.208 | 0.747 \pm 0.116 | 1.090 \pm 0.136 | 29.070 \pm 4.289 |

Western blot assay of **5b** was performed to detect the expression of histone 3 (H3) acetylation which was an important biomarker related to intracellular HDAC1-3 inhibition. MCF-7 cells were treated with compound **5b** and chidamide at 0.25, 2.5, 25 μ M for 24 h to measure the acetylation status of total H3 (**Fig. 4**). As expected, we observed a dose-dependent improvement in the level of Ac-H3 when the cells were incubated with compound **5b**. Not until concentration of 25 μ M was used was an apparent increase in histone H3 acetylation visible for chidamide. This might partly be contributing to a relatively higher biochemical IC_{50} value of chidamide against class I HDACs.

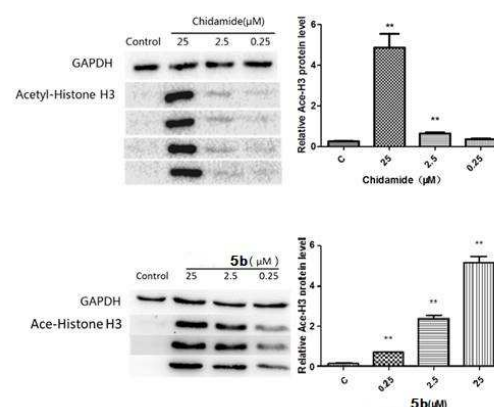


Fig 4. Effect of histone H3 acetylation in breast cancer cell line (MCF-7) by chidamide and **5b** respectively. Cells were treated with **5b** and chidamide for 24 h and followed by western blot analysis.

Further screening for antiproliferative activity of **5b** against a set of 59 solid or hematological tumor cell lines was carried out in NCI (termed NCI-60). The human tumor cell lines of the NCI-60 are some of the most representative cell lines used in laboratory which come from different tissue origins including blood, lung, colon,

central nervous system (CNS), melanoma, ovary, kidney, prostate and breast. Concretely, **5b** was screened at 10 μ M, and cell viability was assessed after 2 days of treatment. As shown in **Table 5**, compound **5b** displayed notable antiproliferative potential against human leukemia cell lines, and all the IRs of which were above 50%, in particular CCRF-CEM and HL60 (TB) with IRs of 84.48% and 84.01%. However, a bad antiproliferation profile was observed for the most solid tumor cell lines, although several exceptions like NCI-H522 (lung cancer), HCT116 (colon cancer) and TK-10 (renal cancer) also exhibited moderate cellular activities with IRs of 70.66%, 73.27% and 72.33% respectively. It appeared that the current HDACs inhibitors including **5b** are more inclined to treat hematological tumors compared with solid tumors.

Table 5.

In vitro antiproliferative screening of compound **5b** (Inhibition rate% at 10 μ M concentration)

| Origin of cancer | Cell line | IR % ^a | Origin of cancer | Cell line | IR % |
|------------------|-----------|-------------------|------------------|-----------------|-------|
| Leukemia | CCRF-CEM | 84.48 | | M14 | 29.39 |
| | HL60 (TB) | 84.01 | | MDA-MB-435 | 28.84 |
| | K562 | 61.56 | | SK-MEL-2 | 52.05 |
| | MOLT-4 | 63.05 | | SK-MEL-28 | 33.76 |
| | RPMI-8226 | 59.78 | | SK-MEL-5 | 34.74 |
| | SR | 57.61 | | UACC-257 | 36.56 |
| Non-Small Cell | A549/ATCC | 12.19 | Ovarian Cancer | UACC-62 | 57.78 |
| Lung Cancer | EKVX | 11.68 | | IGROV1 | 22.82 |
| | HOP-62 | 29.93 | | OVCAR-3 | 41.95 |
| | HOP-92 | 58.58 | | OVCAR-4 | 21.34 |
| | NCI-H226 | 30.21 | | OVCAR-5 | 36.41 |
| | NCI-H23 | 26.46 | | OVCAR-8 | 55.90 |
| Colon Cancer | NCI-H322M | 14.19 | Renal Cancer | NCI/ADR-RES | 18.02 |
| | NCI-H460 | 26.75 | | SK-OV-3 | 29.54 |
| | NCI-H522 | 70.66 | | 786-0 | 7.02 |
| | COLO 205 | 27.8 | | A498 | 47.14 |
| | HCC-2998 | 20.41 | | ACHN | 15.04 |
| | HCT-116 | 73.27 | | RXF 393 | 17.53 |
| | HCT-15 | 0.12 | Prostate Cancer | SN12C | 30.75 |
| | HT29 | 40.35 | | TK-10 | 72.33 |
| | KM12 | 26.91 | | UO-31 | 50.08 |
| | SW-620 | 40.14 | | PC-3 | 39.35 |
| CNS Cancer | SF-268 | 35.98 | Breast Cancer | DU-145 | 13.04 |
| | SF-295 | 16.23 | | MCF7 | 35.53 |
| | SF-539 | 44.80 | | MDA-MB-231/ATCC | 22.42 |
| | SNB-19 | 13.55 | | HS 578T | 29.27 |
| | SNB-75 | 30.64 | | BT-549 | 6.06 |
| | U251 | 35.89 | | T-47D | 58.17 |
| Melanoma | LOX IMVI | 15.71 | | MDA-MB-468 | 9.71 |
| | MALME-3M | 52.58 | | | |

^aIR% was calculated by 100%-growth %, the values of cell growth percent were provided by NCI-60 program.

2.4 Docking study

The molecular docking study was performed with compound **5b** in the catalytic pocket of human HDAC1 crystallographic structure (PDB code: 5ICN) to further rationalize the SAR of isoindolinones. As illustrated in **Fig.5(A)**, the phenyl linker of **5b** could insert into the narrow channel of the binding site and form a π - π stacking interaction with the residues of amino acids Phe150 and Phe205. The amino of the 2-aminobenzamide ZBG group formed a key H-bond with Asp176, and the H atom of the amide between the phenyl linker and ZBG also generated an H-bond interaction with carbonyl of Gly149. These H-bond forces positioned **5b** in a suitable space-conformation to efficiently contact with the zinc atom. Additionally, although isoindolinone core occupied the surface groove which was adjacent to the solvent region, it was surrounded by hydrophobic residues including Ile305, Tyr303, Leu271 and Pro29. This might be responsible for the poor HDAC1 inhibition of azaisoindolinones.

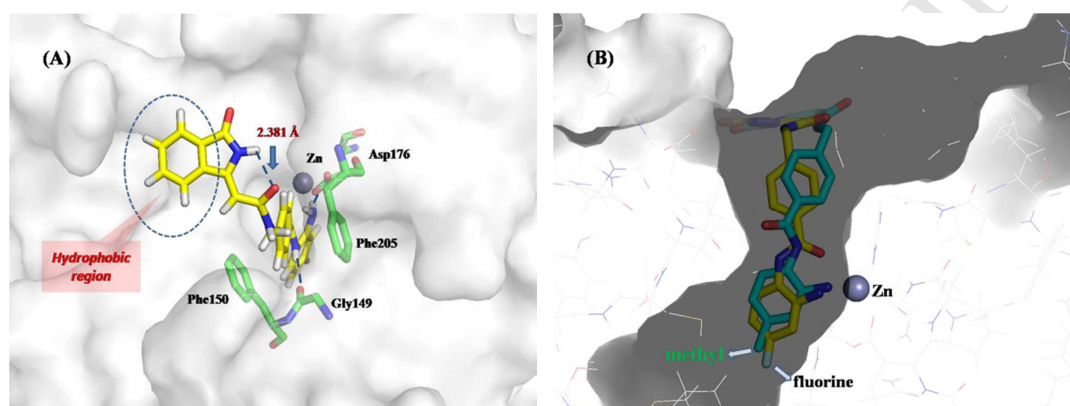


Fig. 5 Docking models of isoindolinone analogues in complex with the HDAC1 catalytic domain. (A) Docking model of **5b** (yellow) in the binding pocket, with key residues in the hydrophobic channel labeled in cyan. The H-bonding interactions with residues were labeled in blue. Zinc ion was labeled in brown. (B) Docked positions obtained for **5b** (yellow) and **5d** (green) in HDAC1 pocket. Methyl substituent was marked with a cyan label and F substituent was marked with a black label. The HDAC1 protein is displayed as a surface representation in gray for clarity.

It should be noted that the distance between H atom of the amide in isoindolinone scaffold and the oxygen atom of the carbonyl linked to the methylene was only 2.381 Å which indicated a potential H-bond formation. This conclusion might also be confirmed by the X-ray crystallography of (Z)3-methyleneisoindolin-1-one in our previous article[28]. The approximately tricyclic capping group of compound **5b** further enhanced the interaction with the large surface of pocket which resulted in the excellent HDAC1 activity and isoforms selectivity of isoindolinones. Additionally, comparing the binding models of **5b** and **5d** (**Fig. 5B**), it appeared that the sterical hindrance between the methyl substituent on ZBG and nearby residues made **5d** in a adverse position close chelate with the zinc ion. This poor combination was probably responsible for the terrible HDAC1 inhibition as exemplified by **5c** and **5d**.

2.5 *In vitro* metabolic stability

In view of the promising results gained from the biological activity assays *in vitro*, a preliminary investigation for metabolic stability of compound **5b** was conducted to determinate half-life ($T_{1/2}$) and CL_{int} in liver microsomes (LMs) from male SD rats, dogs, and human. As shown in **Table 6**, the elimination half-life ($T_{1/2}$) value of **5b** was 292 min in human LM, a bit better than that of chidamide (276 min), whereas shorter $T_{1/2}$ values in dog and rat LMs were observed for **5b** (201 and 121 min) than chidamide (302 min and 190 min). The CL_{int} s of compound **5b** were calculated as 4.80, 6.92 and 11.7 $\mu\text{L} \times \text{min}^{-1} \times \text{mg}^{-1}$ in human, dog, rat LMs correspondingly. This result inspired us to perform further pharmacokinetic studies *in vivo* for **5b**.

Table 6In vitro stabilities of compound **5b** and Chidamide toward human, dog, rat liver microsomes.

| Compound | human | | dog | | rat | |
|-----------|-----------------|------------|-----------------|------------|-----------------|------------|
| | $T_{1/2}$ (min) | CL_{int} | $T_{1/2}$ (min) | CL_{int} | $T_{1/2}$ (min) | CL_{int} |
| 5b | 292 | 4.80 | 201 | 6.92 | 121 | 11.7 |
| Chidamide | 276 | 4.98 | 302 | 5.76 | 190 | 10.35 |

2.6 Pharmacokinetic studies

The pharmacokinetic studies of **5b** were evaluated in SD rats following intravenous administration at 1mg/kg body weight and oral administration at 10 mg/kg body weight. Blood samples were taken, and the plasma was detected for the concentrations of **5b** by an LC-MS/MS system. As illustrated in **Table 7**, **5b** showed a plasma clearance of $21.3 \text{ mL} \cdot \text{kg}^{-1} \cdot \text{min}^{-1}$ with terminal phase elimination half-life ($T_{1/2}$) of 0.39 h administered iv in rats, whereas oral administration in rats gave half-time ($T_{1/2}$) of 1.30 h. The oral bioavailability of 16% suggested that **5b** could be further investigated and optimized as a novel class I HDACs inhibitor.

Table 7Pharmacokinetic parameters of **5b** tested in SD rats.

| Compound | 5b | |
|---|-----------|--------|
| | iv | po |
| route | iv | po |
| Dose (mg/kg) | 1 | 10 |
| CL ($\text{mL} \cdot \text{kg}^{-1} \cdot \text{min}^{-1}$) | 21.3 | / |
| V_{dss} ($\text{L} \cdot \text{kg}^{-1}$) | 0.493 | / |
| AUC_{0-inf} ($\text{ng} \cdot \text{h} \cdot \text{mL}^{-1}$) | 784 | 1742.7 |
| AUC_{0-t} ($\text{ng} \cdot \text{h} \cdot \text{mL}^{-1}$) | 781 | 1710.5 |
| $T_{1/2}$ (h) | 0.39 | 1.30 |
| F (%) | / | 16 |

3. Conclusion

In summary, we have developed a series of novel isoindolinone-based HDACs inhibitor, and evaluated their in vitro activity. Twelve compounds exhibited nanomolar IC_{50} values on HDAC1 inhibition, and the best compounds were **5a** (65.6 nM), **5b** (65.1 nM) and **13a** (57.9 nM). Among these, compound **5b** as a class I HDACs inhibitor displayed superior enzymatic activity than chidamide and an excellent isoforms selectivity profile. **5a** and **5b** also demonstrated nanomolar antiproliferative activities against human Leukemia cell lines HL-60, K562 and colon cell line HCT116, whereas a micromolar effect was observed in breast cancer cell line MCF-7. In comparison of the antiproliferative results of **5a**, **5b** and chidamide, compound **5b** had an overall superior activity against the four cell lines.

Through the NCI antiproliferative screening toward 59 cell lines involving nine tumor types, compound **5b** inhibited the growth of leukemia cell lines, but showed weak antiproliferative activities against most of the solid tumors. The following stability evaluation in LMs (human, dog and rat) indicated that **5b** possessed a better stability in HLM than chidamide. In the case of pharmacokinetic, **5b** showed moderate oral bioavailability of 16% in rats. The in vivo pharmacological assay is currently under investigation in our group.

4. Experimental section**4.1 Chemistry**

All reagents and solvents were reagent grade or were purified by standard methods in advance. Isolation and

purification of the compounds were performed by flash column chromatography on silica gel 60 (230-400 mesh). Analytical thin-layer chromatography (TLC) was conducted on fluka TLC plates (silica gel 60 F254, aluminum foil). The structures of synthesized compounds were characterized by ^1H NMR, ^{13}C NMR and MS. The structural information and detailed synthetic process for the intermediates and target compounds are shown in this section. Melting points were measured using an X-4 melting-point apparatus with a microscope (Beijing Tech Instrument) and were not corrected. ^1H and ^{13}C NMR spectra were recorded in $\text{DMSO}-d_6$ by a 300 MHz spectrometer: chemical shifts (δ) are given in parts per million, coupling constants (J) in Hz. MS were determined by a Nicolet 2000 FT-IR mass spectrometer and MAT-212 mass spectrometer. All of the target compounds were examined by HPLC, and the purity of every case was $\geq 95\%$. Reverse-phase HPLC was performed on an Agilent Technologies 1260 Infinity, which was equipped with a C18 column (Agilent Zorbax SB-C18, 5 μM , 4.6 $\text{mm} \times 150 \text{ mm}$). Mobile phase A was water, and mobile phase B was methanol. A gradient of 20–80% B was run at a flow rate of 0.8 mL/min over 30 min.

4.1.1 General procedure for the preparation of isoindolin scaffolds **1**, **21** and **23a-b**.

To the solution of ethyl propiolate (35.3 mg, 0.36 mmol) and *N*-hydroxyphthalimide (0.3 mmol) in dry DMF (3 mL) was added Bu_3P (15.7 mg, 0.06 mmol). The resulting mixture was heated to 150 $^\circ\text{C}$ under a nitrogen atmosphere for the required period of time. After completion of the reaction as monitored by TLC, the reaction mixture was quenched with CH_2Cl_2 (15 mL), which was washed with water and brine successively, dried over MgSO_4 , filtered, and concentrated in vacuo. Purification by flash chromatography (SiO_2 ; ethyl acetate/PE, 1:10–1:3) yielded the desired products.

4.1.1.1 Ethyl (Z)-2-(3-oxoisoindolin-1-ylidene)acetate (1). 95% isolated yield; white solid. Mp: 167–169 $^\circ\text{C}$. ^1H NMR (300 MHz, $\text{DMSO}-d_6$) δ : 10.95 (s, 1H), 8.98 (d, $J = 7.6 \text{ Hz}$, 1H), 7.91–7.60 (m, 3H), 5.80 (s, 1H), 4.21 (q, $J = 7.1 \text{ Hz}$, 2H), 1.28 (t, $J = 7.1 \text{ Hz}$, 3H). ^{13}C NMR (75 MHz, $\text{DMSO}-d_6$) δ : 167.4, 165.5, 148.0, 133.6, 133.0, 131.7, 131.2, 127.6, 122.7, 98.2, 59.8, 14.1. ESIHRMS: Calcd for $\text{C}_{12}\text{H}_{12}\text{NO}_3$: ($\text{M}+\text{H}$) $^+$ 218.0812. Found: m/z 218.0815.

4.1.1.2 Ethyl (Z)-2-(5,6-dichloro-3-oxoisoindolin-1-ylidene)acetate (21). 90% isolated yield; yellow solid. Mp: 194–196 $^\circ\text{C}$. ^1H NMR (300 MHz, $\text{DMSO}-d_6$) δ : 10.53 (s, 1H), 8.49 (s, 1H), 8.01 (s, 1H), 6.20 (s, 1H), 4.21 (q, $J = 6.9 \text{ Hz}$, 2H), 1.26 (t, $J = 7.0 \text{ Hz}$, 3H). ^{13}C NMR (75 MHz, $\text{DMSO}-d_6$) δ : 167.9, 167.7, 146.4, 138.3, 137.9, 136.3, 130.8, 127.0, 126.3, 95.9, 62.0, 16.0. ESIHRMS: Calcd for $\text{C}_{12}\text{H}_9\text{Cl}_2\text{N}_1\text{NaO}_3$: ($\text{M}+\text{Na}$) $^+$ 307.9852. Found: m/z 307.9857.

4.1.1.3 Ethyl (Z)-2-(5-oxo-5,6-dihydro-7H-pyrrolo[3,4-*b*]pyridin-7-ylidene)acetate (23a). 45% isolated yield; black solid. Mp: 128–130 $^\circ\text{C}$. ^1H NMR (300 MHz, $\text{DMSO}-d_6$) δ : 10.79 (s, 1H), 8.90 (dd, $J_1 = 4.9 \text{ Hz}$, $J_2 = 1.5 \text{ Hz}$, 1H), 8.26 (dd, $J_1 = 7.7 \text{ Hz}$, $J_2 = 1.5 \text{ Hz}$, 1H), 7.70 (dd, $J_1 = 7.7 \text{ Hz}$, $J_2 = 4.9 \text{ Hz}$, 1H), 5.99 (s, 1H), 4.24 (q, $J = 7.1 \text{ Hz}$, 2H), 1.27 (t, $J = 7.1 \text{ Hz}$, 3H); ESI-MS m/z : 219.1 [$\text{M}+\text{H}$] $^+$.

4.1.1.4 Ethyl (Z)-2-(7-oxo-6,7-dihydro-5H-pyrrolo[3,4-*b*]pyridin-5-ylidene)acetate (23b). 45% isolated yield; black solid. Mp: 125–127 $^\circ\text{C}$. ^1H NMR (300 MHz, $\text{DMSO}-d_6$) δ : 10.79 (s, 1H), 8.88 (dd, $J_1 = 4.8 \text{ Hz}$, $J_2 = 1.4 \text{ Hz}$, 1H), 8.57 (dd, $J_1 = 7.9 \text{ Hz}$, $J_2 = 1.4 \text{ Hz}$, 1H), 7.73 (dd, $J_1 = 7.9 \text{ Hz}$, $J_2 = 4.8 \text{ Hz}$, 1H), 6.22 (s, 1H), 4.23 (q, $J = 7.1 \text{ Hz}$, 2H), 1.28 (t, $J = 7.1 \text{ Hz}$, 3H); ESI-MS m/z : 241.1 [$\text{M}+\text{Na}$] $^+$.

4.1.2 General procedure for the preparation of isoindolin scaffolds **15a-c**

Substituted nitriles (0.5 mmol, 1.0 equiv), [$\{\text{RuCl}_2(p\text{-cymene})\}_2$] (0.025 mmol, 5 mol %), $\text{Cu}(\text{OAc})_2 \cdot \text{H}_2\text{O}$ (1.0

mmol, 2.0 equiv), AgSbF₆ (0.10 mmol, 20 mol %) were taken in a 15 mL pressure tube equipped with a magnetic stirrer and septum. To the tube were then added liquid alkene (2.0 mmol, 4.0 equiv) and acetic acid solvent (3 mL) via syringes, allowed the reaction mixture to stir at room temperature for few seconds. Then, the septum was taken out and immediately a screw cap was used to cover the tube. The reaction mixture was allowed to stir at 120 °C. Then, the reaction was monitored by TLC until the maximum conversion. The reaction mixture was diluted with CH₂Cl₂, filtered through Celite and silica gel, and the filtrate was concentrated. The crude residue was purified through a silica gel column using hexanes and ethyl acetate as eluent to give pure **15a-c**.

4.1.2.1 Ethyl (Z)-2-(6-fluoro-3-oxoisindolin-1-ylidene)acetate (15a). 23% isolated yield; white solid. Mp: 169-171 °C. ¹H NMR (300 MHz, DMSO-*d*₆) δ: 10.47 (s, 1H), 8.08 (dd, *J*₁ = 2.1 Hz, *J*₂ = 8.8 Hz, 1H), 7.86 (m, 1H), 7.52 (m, 1H), 6.18 (s, 1H), 4.22 (q, *J* = 7.1 Hz, 2H), 1.27 (t, *J* = 7.1 Hz, 3H); ESI-MS *m/z*: 236.1 [M+H]⁺.

4.1.2.2 Ethyl (Z)-2-(3-oxo-6-(trifluoromethyl)isindolin-1-ylidene)acetate (15b). 20% isolated yield; white solid. Mp: 170-172 °C. ¹H NMR (300 MHz, DMSO-*d*₆) δ: 10.75 (s, 1H), 8.66 (s, 1H), 8.03 (s, 2H), 6.41 (s, 1H), 4.23 (q, *J* = 7.1 Hz, 2H), 1.28 (t, *J* = 7.1 Hz, 3H); ESI-MS *m/z*: 308.1 [M+Na]⁺.

4.1.2.3 Ethyl (Z)-2-(6-methoxy-3-oxoisindolin-1-ylidene)acetate (15c). 25% isolated yield; white solid. Mp: 175-177 °C. ¹H NMR (300 MHz, DMSO-*d*₆) δ: 10.17 (s, 1H), 7.77 (m, 2H), 7.23 (m, 1H), 6.20 (s, 1H), 4.26 (q, *J* = 7.0 Hz, 2H), 3.93 (s, 1H), 1.31 (t, *J* = 7.1 Hz, 3H); ESI-MS *m/z*: 248.2 [M+Na]⁺.

4.1.3 Tert-butyl (2-amino-4-fluorophenyl)carbamate (8).

A round-bottom flask charged with 4-fluorobenzene-1, 2-diamine **7** (126 mg, 1 mmol) and KHCO₃ (200 mg, 2 mmol) was taken up in CH₃CN at 0 °C. After 5 min, (Boc)₂O (0.23 mL, 1mmol) was added in portions and the resulting mixture was stirred overnight. Then, the mixture was concentrated and extracted with EtOAc. The combined organic extracts were washed with brine, dried over anhydrous Na₂SO₄ and concentrated in vacuo. The product obtained by chromatography on a silica gel column. 90% isolated yield; white solid; Mp: 95-97 °C. ¹H NMR (300 MHz, DMSO-*d*₆) δ: 8.18 (s, 1H), 7.22-7.07 (m, 1H), 6.45 (dd, *J*₁ = 2.85 Hz, *J*₂ = 11.13 Hz, 1H), 6.28 (td, *J*₁ = 2.88 Hz, *J*₂ = 8.55 Hz, 1H), 5.10 (s, 2H), 1.44 (s, 9H); ESI-MS *m/z*: 227.1 [M+H]⁺.

4.1.4 General procedure for the hydrolysis of esters to yield various acids

To a solution of various esters (1 mmol) in MeOH and H₂O (10 mL, v/v = 1: 1) was added Lithium hydroxide (95.8 mg, 4 mmol) at 0 °C. Then, mixture was allowed to stir at room temperature. The reaction was monitored by TLC until the maximum conversion. After neutralized with acetic acid, the formed precipitate was collected by filtration, washed with water, and dried in vacuo to give the title compounds

4.1.4.1 (Z)-2-(3-oxoisindolin-1-ylidene)acetic acid (2). 90.2% isolated yield; white solid. Mp: 218-220 °C. ¹H NMR (300 MHz, DMSO-*d*₆) δ: 12.06 (brs, 1H), 10.90 (s, 1H), 8.99 (d, *J* = 7.6 Hz, 1H), 7.92-7.63 (m, 3H), 5.82 (s, 1H). ESI-MS *m/z*: 190.2 [M+H]⁺.

4.1.4.2 (Z)-4-((2-(3-oxoisindolin-1-ylidene)acetamido)methyl)benzoic acid (4). 95% isolated yield; white solid. Mp: 205-207 °C. ¹H NMR (300 MHz, DMSO-*d*₆) δ: 12.83 (brs, 1H), 10.39 (s, 1H), 8.89 (s, 1H), 7.92 (d, *J* = 7.77 Hz, 2H), 7.87-7.71 (m, 4H), 7.43 (d, *J* = 7.77 Hz, 2H), 6.10 (s, 1H), 4.49 (d, *J* = 5.58 Hz, 2H); ESI-MS *m/z*: 321.1 [M+H]⁺.

4.1.4.3 (Z)-2-(5-oxo-5,6-dihydro-7H-pyrrolo[3,4-b]pyridin-7-ylidene)acetic acid (**24a**). 84% isolated yield; black solid. Mp: 142–156 °C. ¹H NMR (300 MHz, DMSO-*d*₆) δ : 12.83 (brs, 1H), 10.89 (s, 1H), 8.93 (dd, $J_1 = 4.9$ Hz, $J_2 = 1.5$ Hz, 1H), 8.28 (dd, $J_1 = 7.7$ Hz, $J_2 = 1.5$ Hz, 1H), 7.73 (dd, $J_1 = 7.7$ Hz, $J_2 = 4.9$ Hz, 1H), 5.98 (s, 1H); ESI-MS *m/z*: 219.1 [M+H]⁺.

4.1.4.4 (Z)-2-(7-oxo-6,7-dihydro-5H-pyrrolo[3,4-b]pyridin-5-ylidene)acetic acid (**24b**). 87% isolated yield; black solid. Mp: 138–140 °C. ¹H NMR (300 MHz, DMSO-*d*₆) δ : 12.83 (brs, 1H), 10.88 (s, 1H), 8.98 (dd, $J_1 = 4.8$ Hz, $J_2 = 1.4$ Hz, 1H), 8.59 (dd, $J_1 = 7.9$ Hz, $J_2 = 1.4$ Hz, 1H), 7.77 (dd, $J_1 = 7.9$ Hz, $J_2 = 4.8$ Hz, 1H), 6.28 (s, 1H); ESI-MS *m/z*: 191.1 [M+H]⁺.

4.1.4.5 (Z)-6-(2-(3-oxoisindolin-1-ylidene)acetamido)hexanoic acid (**11a**). 71% isolated yield; white solid. Mp: 178–180 °C; ¹H NMR (300 MHz, DMSO-*d*₆) δ : 11.88 (brs, 1H), 10.44 (s, 1H), 8.35 (t, $J = 5.5$ Hz, 1H), 7.85–7.80 (m, 2H), 7.78–7.73 (m, 1H), 7.69–7.64 (m, 1H), 6.02 (s, 1H), 3.23–3.16 (m, 2H), 2.32 (t, $J = 7.4$ Hz, 2H), 1.60–1.42 (m, 4H), 1.36–1.28 (m, 2H); ESI-MS *m/z*: 340.1 [M+Na]⁺.

4.1.4.6 (Z)-7-(2-(3-oxoisindolin-1-ylidene)acetamido)heptanoic acid (**11b**). 79% isolated yield; white solid. Mp: 180–182 °C. ¹H NMR (300 MHz, DMSO-*d*₆) δ : 11.89 (brs, 1H), 10.44 (s, 1H), 8.36 (t, $J = 5.5$ Hz, 1H), 7.84–7.73 (m, 3H), 7.68 (m, 1H), 6.01 (s, 1H), 3.22–3.16 (m, 2H), 2.23 (t, $J = 7.3$ Hz, 2H), 1.59–1.38 (m, 4H), 1.30 (s, 4H); ESI-MS *m/z*: 317.4 [M+H]⁺.

4.1.4.7 (Z)-2-(6-fluoro-3-oxoisindolin-1-ylidene)acetic acid (**16a**). 63% isolated yield; white solid. Mp: 189–191 °C. ¹H NMR (300 MHz, DMSO-*d*₆) δ : 11.89 (brs, 1H), 10.48 (s, 1H), 8.09 (dd, $J_1 = 2.1$ Hz, $J_2 = 8.8$ Hz, 1H), 7.88 (m, 1H), 7.54 (m, 1H), 6.19 (s, 1H); ESI-MS *m/z*: 208.2 [M+H]⁺.

4.1.4.8 (Z)-2-(6-trifluoromethyl-3-oxoisindolin-1-ylidene)acetic acid (**16b**). 60% isolated yield; white solid; Mp: 178–180 °C. ¹H NMR (300 MHz, DMSO-*d*₆) δ : 11.91 (brs, 1H), 10.76 (s, 1H), 8.67 (s, 1H), 8.04 (s, 2H), 6.42 (s, 1H); ESI-MS *m/z*: 258.2 [M+H]⁺.

4.1.4.9 (Z)-2-(6-methoxy-3-oxoisindolin-1-ylidene)acetic acid (**16c**). 68% isolated yield; white solid. Mp: 185–187 °C. ¹H NMR (300 MHz, DMSO-*d*₆) δ : 11.91 (brs, 1H), 10.18 (s, 1H), 7.78 (m, 2H), 7.23 (m, 1H), 6.22 (s, 1H), 3.94 (s, 1H); ESI-MS *m/z*: 220.2 [M+H]⁺.

4.1.4.10 (Z)-4-((2-(5-oxo-5,6-dihydro-7H-pyrrolo[3,4-b]pyridin-7-ylidene)acetamido)methyl)benzoic acid (**26a**). 69% isolated yield; black solid. Mp: 158–160 °C. ESI-MS *m/z*: 346.3 [M+H]⁺. ¹H NMR (300 MHz, DMSO-*d*₆) δ : 12.71 (s, 1H), 10.79 (s, 1H), 9.07 (s, 1H), 8.91 (dd, $J_1 = 4.8$ Hz, $J_2 = 1.4$ Hz, 1H), 8.25 (dd, $J_1 = 7.7$ Hz, $J_2 = 1.4$ Hz, 1H), 7.77–7.70 (m, 5H), 5.98 (s, 1H), 4.54 (d, $J = 5.7$ Hz, 2H).

4.1.4.11 (Z)-4-((2-(7-oxo-6,7-dihydro-5H-pyrrolo[3,4-b]pyridin-5-ylidene)acetamido)methyl)benzoic acid (**26b**). 71% isolated yield; black solid. Mp: 158–160 °C. ESI-MS *m/z*: 346.3 [M+H]⁺. ¹H NMR (300 MHz, DMSO-*d*₆) δ : 12.70 (s, 1H), 10.79 (s, 1H), 9.08 (s, 1H), 8.89 (dd, $J_1 = 4.9$ Hz, $J_2 = 1.6$ Hz, 1H), 8.57 (dd, $J_1 = 7.9$ Hz, $J_2 = 1.4$ Hz, 1H), 7.81–7.71 (m, 5H), 6.24 (s, 1H), 4.43 (d, $J = 5.9$ Hz, 2H).

4.1.5 General procedure for the amidation of various acids with various amides

To a solution of acid (1 mmol) was added DIPEA (0.66 mL, 4 mmol), HATU (353.2 mg, 1.1 mmol) and

DMF (10 mL) at 0 °C. After 30 min, various amides (1mmol) were added. The mixture was stirred for 6 h. After completion of the reaction as monitored by TLC, the mixture was poured into water (30 mL) and extracted with EtOAc (3×30 mL). The combined organic extracts were washed with brine (2×30 mL), dried over anhydrous Na₂SO₄ and concentrated in vacuo. The product was obtained by chromatography on a silica gel column.

4.1.5.1 Methyl (Z)-4-((2-(3-oxoisindolin-1-ylidene)acetamido)methyl)benzoate (3). 74% isolated yield; white solid. Mp: 156-158 °C. ¹H NMR (300 MHz, DMSO-*d*₆) δ: 10.40 (s, 1H), 8.92 (s, 1H), 7.95 (d, *J* = 9.00 Hz, 2H), 7.85-7.70 (m, 4H), 7.46 (d, *J* = 8.13 Hz, 2H), 6.10 (s, 1H), 4.50 (d, *J* = 5.64 Hz, 2H), 3.85 (s, 1H); ESI-MS *m/z*: 358.1 [M+Na]⁺.

4.1.5.2 (Z)-N-(2-aminophenyl)-4-((2-(3-oxoisindolin-1-ylidene)acetamido)methyl)benzamide (5a). 35% isolated yield; white solid. Mp: 179-180 °C; ¹H NMR (300 MHz, DMSO-*d*₆) δ: 10.43 (s, 1H), 9.65 (s, 1H), 8.94 (t, *J* = 5.88 Hz, 1H), 7.96 (d, *J* = 8.07 Hz, 2H), 7.88-7.74 (m, 3H), 7.70-7.68 (m, 1H), 7.43 (d, *J* = 7.65 Hz, 2H), 7.16 (d, *J* = 7.59 Hz, 1H), 6.99-6.94 (m, 1H), 6.79-6.76 (m, 1H), 6.60 (m, 1H), 6.11 (s, 1H), 4.90 (s, 2H), 4.49 (d, *J* = 5.85 Hz, 2H); ¹³C NMR (75 MHz, DMSO-*d*₆) δ: 167.26, 166.26, 165.08, 143.14, 143.10, 142.70, 136.48, 133.26, 132.97, 131.22, 128.90, 127.87, 127.80, 126.63, 126.43, 123.33, 123.28, 121.00, 116.25, 116.12, 95.17, 41.93; ESI-MS *m/z*: 435.1 [M+Na]⁺.

4.1.5.3 (Z)-N-(2-amino-4-fluorophenyl)-4-((2-(3-oxoisindolin-1-ylidene)acetamido)methyl)benzamide (5b). 37% isolated yield; white solid. Mp: 208-209 °C; ¹H NMR (300 MHz, DMSO-*d*₆) δ: 10.44 (s, 1H), 9.58 (s, 1H), 8.95 (t, *J* = 5.88 Hz, 1H), 7.96 (d, *J* = 8.07 Hz, 2H), 7.84-7.77 (m, 3H), 7.74-7.68 (m, 1H), 7.43 (d, *J* = 8.07 Hz, 2H), 7.13-7.08 (m, 1H), 6.54 (dd, *J*₁ = 2.7 Hz, *J*₂ = 11.2 Hz, 1H), 6.35 (dd, *J*₁ = 2.7 Hz, *J*₂ = 8.6 Hz, 1H), 6.11 (s, 1H), 5.23 (s, 2H), 4.49 (d, *J* = 5.85 Hz, 2H); ESI-MS *m/z*: 429.2 [M+H]⁺. ¹³C NMR (75 MHz, DMSO-*d*₆) δ: 167.24, 166.26, 165.15, 143.15, 142.96, 138.83, 136.43, 132.97, 133.00, 131.23, 128.90, 127.91, 127.10, 123.28, 121.00, 116.58, 112.57, 112.38, 112.29, 112.06, 95.14, 41.93. ESI-MS *m/z*: 431.4 [M+H]⁺.

4.1.5.4 (Z)-N-(2-amino-4-chlorophenyl)-4-((2-(3-oxoisindolin-1-ylidene)acetamido)methyl)benzamide (5c). 31% isolated yield; white solid. Mp: 160-162 °C; ¹H NMR (300 MHz, DMSO-*d*₆) δ: 10.43 (s, 1H), 9.64 (s, 1H), 8.94 (s, 1H), 7.95 (d, *J* = 8.16 Hz, 2H), 7.88-7.68 (m, 5H), 7.43 (d, *J* = 8.16 Hz, 2H), 6.80 (m, 1H), 6.10 (s, 1H), 5.18 (m, 2H), 4.49 (d, *J* = 5.85 Hz); ¹³C NMR (75 MHz, DMSO-*d*₆) δ: 167.78, 166.74, 165.79, 145.30, 143.64, 143.35, 136.98, 133.55, 133.49, 129.40, 128.75, 128.45, 127.54, 123.80, 122.47, 121.52, 115.87, 115.26, 95.66, 42.42. ESI-MS *m/z*: 469.1 [M+Na]⁺.

4.1.5.5 (Z)-N-(2-amino-4-methylphenyl)-4-((2-(3-oxoisindolin-1-ylidene)acetamido)methyl)benzamide (5d). 29% isolated yield; white solid. Mp: 145-146 °C; ¹H NMR (300 MHz, DMSO-*d*₆) δ: 10.43 (s, 1H), 9.58 (s, 1H), 8.94 (s, 1H), 7.95 (d, *J* = 8.10 Hz, 2H), 7.88-7.68 (m, 4H), 7.42 (d, *J* = 8.10 Hz, 2H), 7.01 (d, *J* = 8.10 Hz, 1H), 6.58 (s, 1H), 6.41 (d, *J* = 7.92 Hz, 1H), 6.10 (s, 1H), 4.81 (s, 2H), 4.49 (d, *J* = 5.85 Hz, 2H), 2.17 (s, 3H); ¹³C NMR (75 MHz, DMSO-*d*₆) δ: 167.78, 166.74, 165.54, 143.63, 143.35, 143.14, 136.98, 135.98, 133.79, 133.49, 131.75, 129.39, 128.36, 127.53, 127.08, 123.80, 121.53, 121.40, 117.63, 117.04, 95.68, 42.41. ESI-MS *m/z*: 449.2 [M+Na]⁺.

4.1.5.6 Tert-butyl (Z)-4-(4-fluoro-2-(4-((2-(3-oxoisindolin-1-ylidene)acetamido)methyl)benzamido)Phenyl)carbamate (9). 72% isolated yield; white solid. Mp: 168-170 °C; ¹H NMR (300 MHz, DMSO-*d*₆) δ: 10.40 (s, 1H), 9.79 (s, 1H), 8.92 (s, 1H), 8.75 (s, 1H), 7.92 (d, *J* = 8.13 Hz, 2H), 7.89-7.72 (m, 3H), 7.72-7.63 (m, 1H), 7.58-7.41 (m, 4H),

7.07-7.01 (m, 1H), 6.11 (s, 1H), 4.51 (d, $J = 5.7$ Hz, 2H), 1.44 (s, 9H); ESI-MS m/z : 553.2 $[M+Na]^+$.

4.1.5.7 Methyl (Z)-6-(2-(3-oxoisindolin-1-ylidene)acetamido)hexanoate (10a). 82% isolated yield; white solid. Mp: 120–122 °C. 1H NMR (300 MHz, DMSO- d_6) δ : 10.43 (s, 1H), 8.35 (t, $J = 5.5$ Hz, 1H), 7.85-7.80 (m, 2H), 7.78-7.73 (m, 1H), 7.69-7.64 (m, 1H), 6.00 (s, 1H), 3.58 (s, 3H), 3.21-3.14 (m, 2H), 2.31 (t, $J = 7.4$ Hz, 2H), 1.60-1.42 (m, 4H), 1.35-1.27 (m, 2H); ESI-MS m/z : 339.1 $[M+Na]^+$.

4.1.5.8 Methyl (Z)-7-(2-(3-oxoisindolin-1-ylidene)acetamido)heptanoate (10b). 91% isolated yield; white solid. Mp: 125–127 °C. 1H NMR (300 MHz, DMSO- d_6) δ : 10.42 (s, 1H), 8.36 (t, $J = 5.5$ Hz, 1H), 7.84-7.73 (m, 3H), 7.67 (m, 1H), 6.01 (s, 1H), 3.57 (s, 3H), 3.21-3.14 (m, 2H), 2.20 (t, $J = 7.3$ Hz, 2H), 1.58-1.35 (m, 4H), 1.29 (s, 4H); ESI-MS m/z : 353.1 $[M+Na]^+$.

4.1.5.9 Methyl (Z)-4-((2-(5-oxo-5,6-dihydro-7H-pyrrolo[3,4-*b*]pyridin-7-ylidene)acetamido)methyl)benzoate (25a). 71% isolated yield; black solid. Mp: 150–152 °C. ESI-MS m/z : 338.3 $[M+H]^+$. 1H NMR (300 MHz, DMSO- d_6) δ : 10.79 (s, 1H), 9.05 (s, 1H), 8.91 (dd, $J_1 = 4.8$ Hz, $J_2 = 1.3$ Hz, 1H), 8.25 (d, $J = 7.5$ Hz, 1H), 7.77-7.70 (m, 5H), 5.99 (s, 1H), 4.53 (d, $J = 5.7$ Hz, 2H), 3.89 (s, 3H).

4.1.5.10 Methyl (Z)-4-((2-(7-oxo-6,7-dihydro-5H-pyrrolo[3,4-*b*]pyridin-5-ylidene)acetamido)methyl)benzoate (25b). 74% isolated yield; black solid. Mp: 151–153 °C. ESI-MS m/z : 338.3 $[M+H]^+$. 1H NMR (300 MHz, DMSO- d_6) δ : 10.79 (s, 1H), 9.06 (s, 1H), 8.88 (dd, $J_1 = 5.0$ Hz, $J_2 = 1.4$ Hz, 1H), 8.57 (dd, $J_1 = 7.9$ Hz, $J_2 = 1.4$ Hz, 1H), 7.81-7.71 (m, 5H), 6.23 (s, 1H), 4.42 (d, $J = 5.8$ Hz, 2H), 3.88 (s, 3H).

4.1.5.11 (Z)-N-(2-amino-4-fluorophenyl)-6-(2-(3-oxoisindolin-1-ylidene)acetamido)hexanamide (12a). 43% isolated yield; white solid. Mp: 188-189 °C; 1H NMR (300 MHz, DMSO- d_6) δ : 10.43 (s, 1H), 9.02 (s, 1H), 8.36 (t, $J = 5.5$ Hz, 1H), 7.84-7.73 (m, 3H), 7.69-7.64 (m, 1H), 7.11-7.06 (m, 1H), 6.50-6.45 (m, 1H), 6.30-6.23 (m, 1H), 6.01 (s, 1H), 5.14 (s, 2H), 3.23-3.17 (m, 2H), 2.33-2.28 (m, 1H), 1.66-1.59 (m, 2H), 1.55-1.46 (m, 2H), 1.41-1.32 (m, 2H); ^{13}C NMR (75 MHz, DMSO- d_6) δ : 171.82, 167.67, 166.57, 144.80, 144.65, 143.04, 137.00, 133.41, 131.61, 129.41, 127.63, 127.50, 123.76, 121.40, 119.99, 96.12, 38.96, 36.05, 29.36, 26.63, 25.43. ESI-MS m/z : 411.2 $[M+H]^+$.

4.1.5.12 (Z)-N-(2-aminophenyl)-6-(2-(3-oxoisindolin-1-ylidene)acetamido)hexanamide (12b). 45% isolated yield; Mp: 179-180 °C; white solid. 1H NMR (300 MHz, DMSO- d_6) δ : 10.44 (s, 1H), 9.10 (s, 1H), 8.35 (s, 1H), 7.97-7.78 (m, 2H), 7.76-7.72 (m, 1H), 7.69-7.65 (m, 1H), 7.13 (d, $J = 13.9$ Hz, 1H), 6.87 (t, $J = 7.1$ Hz, 1H), 6.71 (d, $J = 7.9$ Hz, 1H), 6.52 (t, $J = 7.2$ Hz, 1H), 6.01 (s, 1H), 5.10 (s, 2H), 3.23-3.17 (m, 2H), 2.33-2.28 (m, 1H), 1.66-1.59 (m, 2H), 1.55-1.46 (m, 2H), 1.41-1.32 (m, 2H); ^{13}C NMR (75 MHz, DMSO- d_6) δ : 171.56, 167.68, 166.57, 143.05, 142.37, 137.01, 133.42, 131.61, 129.42, 126.16, 125.78, 124.02, 123.76, 121.41, 116.61, 116.34, 96.13, 38.97, 36.16, 29.36, 26.63, 25.51. ESI-MS m/z : 415.2 $[M+Na]^+$.

4.1.5.13 (Z)-N-(2-amino-4-fluorophenyl)-7-(2-(3-oxoisindolin-1-ylidene)acetamido)heptanamide (12c). 39% isolated yield; white solid. Mp: 189-191 °C; 1H NMR (300 MHz, DMSO- d_6) δ : 10.44 (s, 1H), 9.04 (s, 1H), 8.36 (s, 1H), 7.84-7.78 (m, 2H), 7.75-7.70 (m, 1H), 7.69-7.64 (m, 1H), 7.11-7.06 (m, 1H), 6.50-6.45 (m, 1H), 6.38-6.23 (m, 1H), 6.01 (s, 1H), 5.14 (s, 2H), 3.23-3.16 (m, 2H), 2.33-2.23 (m, 2H), 1.61-1.48 (m, 4H), 1.34 (s, 4H); ^{13}C NMR (75 MHz, DMSO- d_6) δ : 171.86, 167.67, 166.55, 144.78, 144.62, 143.03, 137.00, 133.41, 131.61, 129.41, 127.53, 123.76, 121.39, 120.03, 96.14, 39.01, 36.09, 29.43, 28.89, 26.75, 25.65. ESI-MS m/z : 447.2 $[M+Na]^+$.

4.1.5.14 (Z)-N-(2-aminophenyl)-7-(2-(3-oxoisindolin-1-ylidene)acetamido)heptanamide (**12d**). 42% isolated yield; Mp: 150-151 °C; white solid. ¹H NMR (300 MHz, DMSO-*d*₆) δ: 10.42 (s, 1H), 9.10 (s, 1H), 8.34 (s, 1H), 7.96 – 7.78 (m, 2H), 7.75 (t, *J* = 7.3 Hz, 1H), 7.66 (t, *J* = 7.1 Hz, 1H), 7.13 (d, *J* = 13.9 Hz, 1H), 6.88 (t, *J* = 7.1 Hz, 1H), 6.71 (d, *J* = 7.9 Hz, 1H), 6.53 (t, *J* = 7.2 Hz, 1H), 6.00 (s, 1H), 3.19 (dd, *J* = 12.1, 6.1 Hz, 2H), 2.31 (t, *J* = 7.2 Hz, 2H), 1.60 (s, 2H), 1.48 (s, 2H), 1.34 (s, 3H); ¹³C NMR (75 MHz, DMSO-*d*₆) δ: 171.12, 167.19, 166.05, 142.52, 141.74, 136.51, 132.91, 131.09, 128.91, 125.64, 125.24, 123.62, 123.23, 120.88, 116.22, 115.92, 95.64, 38.52, 35.70, 28.91, 28.36, 26.23, 25.21. ESI-MS *m/z*: 429.3 [M+Na]⁺.

4.1.5.15 (Z)-N-(2-amino-4-fluorophenyl)-4-((2-(6-fluoro-3-oxoisindolin-1-ylidene)acetamido)methyl)benzamide (**20a**). 13% isolated yield; Mp: 158-160 °C; white solid. ¹H NMR (300 MHz, DMSO-*d*₆) δ: 10.50 (s, 1H), 9.60 (s, 1H), 8.99 (t, *J* = 5.3 Hz, 1H), 7.99 (d, *J* = 8.1 Hz, 2H), 7.94-7.89 (m, 1H), 7.83-7.80 (m, 1H), 7.62-7.51 (m, 1H), 7.47 (d, *J* = 8.2 Hz, 2H), 7.20-7.04 (m, 1H), 6.58 (dd, *J* = 11.3, 2.7 Hz, 1H), 6.40 (m, 1H), 6.16 (s, 1H), 5.25 (s, 2H), 4.53 (d, *J* = 5.8 Hz, 2H); ¹³C NMR (75 MHz, DMSO-*d*₆) δ: 167.80, 166.76, 165.81, 145.36, 143.66, 143.33, 136.99, 133.57, 133.50, 131.77, 129.41, 128.77, 128.54, 127.55, 123.90, 122.49, 121.54, 115.89, 115.23, 95.80, 42.43. ESI-MS *m/z*: 449.2 [M+H]⁺.

4.1.5.16 (Z)-N-(2-amino-4-fluorophenyl)-4-((2-(6-trifluoromethyl-3-oxoisindolin-1-ylidene)acetamido)methyl)benzamide (**20b**). 15% isolated yield; Mp: 156-157 °C; white solid. ¹H NMR (300 MHz, DMSO-*d*₆) δ: 10.78 (s, 1H), 9.64 (s, 1H), 8.97 (s, 1H), 8.37 (s, 1H), 8.25 (s, 2H), 8.08-8.00 (m, 2H), 7.49-7.39 (m, 2H), 7.18-7.14 (m, 1H), 6.60 (m, *J* = 11.6 Hz, 1H), 6.43-6.31 (m, 1H), 6.37 (s, 1H), 5.29 (s, 2H), 4.55-4.42 (m, 2H); ¹³C NMR (75 MHz, DMSO-*d*₆) δ: 168.67, 167.68, 166.57, 147.73, 144.58, 144.38, 140.26, 137.98, 134.40, 132.66, 130.33, 129.33, 128.53, 124.71, 122.43, 117.95, 115.66, 113.81, 113.48, 96.56, 42.47. ESI-MS *m/z*: 521.1 [M+Na]⁺.

4.1.5.17 (Z)-N-(2-amino-4-fluorophenyl)-4-((2-(6-methoxy-3-oxoisindolin-1-ylidene)acetamido)methyl)benzamide (**20c**). 16% isolated yield; white solid. Mp: 159-160 °C; ¹H NMR (300 MHz, DMSO-*d*₆) δ: 10.24 (s, 1H), 9.58 (s, 1H), 9.01-8.76 (m, *J* = 5.8 Hz, 1H), 7.95 (d, *J* = 8.0 Hz, 2H), 7.73 (d, *J* = 8.4 Hz, 1H), 7.57-7.33 (m, 3H), 7.26-7.16 (m, 1H), 7.16-7.03 (m, 1H), 6.67-6.47 (m, 1H), 6.44-6.30 (m, 1H), 6.10 (s, 1H), 5.23 (s, 2H), 4.49 (d, *J* = 5.9 Hz, 2H), 3.91 (s, 3H); ¹³C NMR (75 MHz, DMSO-*d*₆) δ: 167.60, 166.80, 165.85, 163.80, 146.01, 143.67, 143.31, 139.43, 133.58, 128.39, 127.45, 125.34, 121.88, 119.74, 118.35, 106.03, 102.66, 102.36, 102.10, 101.77, 95.49, 42.42. ESI-MS *m/z*: 483.2 [M+Na]⁺.

4.1.5.18 (Z)-N-(2-amino-4-fluorophenyl)-4-((2-(5,6-dichloro-3-oxoisindolin-1-ylidene)acetamido)methyl)benzamide (**20d**). 30% isolated yield; white solid. Mp: 140-142 °C; ¹H NMR (300 MHz, DMSO-*d*₆) δ: 10.67 (s, 1H), 9.59 (s, 1H), 8.98 (s, 1H), 8.30 (s, 1H), 8.11 (s, 1H), 7.99 (d, *J* = 7.8 Hz, 2H), 7.46 (d, *J* = 8.2 Hz, 2H), 7.18-7.11 (m, 1H), 6.61-6.56 (m, 1H), 6.43-6.36 (m, 1H), 6.22 (s, 1H), 5.24 (s, 1H), 4.53 (d, *J* = 5.6 Hz, 2H); ¹³C NMR (75 MHz, DMSO-*d*₆) δ: 169.93, 168.88, 167.68, 148.39, 147.42, 143.64, 139.12, 138.12, 135.93, 135.64, 133.90, 131.54, 130.50, 129.68, 129.23, 125.95, 123.67, 123.55, 119.78, 119.18, 97.82, 42.56. ESI-MS *m/z*: 497.1 [M-H]⁻.

4.1.5.19 (Z)-N-(2-amino-4-fluorophenyl)-4-((2-(5-oxo-5,6-dihydro-7H-pyrrolo[3,4-*b*]pyridin-7-ylidene)acetamido)methyl)benzamide (**27a**). 41% isolated yield; white solid. Mp: 232-233 °C; ¹H NMR (300 MHz, DMSO-*d*₆) δ: 10.79 (s, 1H), 9.57 (s, 1H), 9.05 (s, 1H), 8.79 (dd, *J* = 4.9, 1.5 Hz, 1H), 8.13 (dd, *J*₁ = 1.5 Hz, *J*₂ = 7.6 Hz, 1H), 7.92 (d, *J* = 8.1 Hz, 2H), 7.58 (m, 1H), 7.48 (d, *J* = 8.1 Hz, 2H), 7.09 (m, 1H), 6.62 (s, 1H), 6.53 (dd, *J*₁ = 2.8 Hz, *J*₂ = 11.2 Hz, 1H), 6.35 (td, *J*₁ = 8.5 Hz, *J*₂ = 2.7 Hz, 1H), 5.22 (s, 2H), 4.86 (d, *J* = 16.2 Hz, 1H), 4.58 (d, *J* = 16.3 Hz,

1H); ¹³C NMR (75 MHz, DMSO-*d*₆) δ : 166.63, 165.34, 164.86, 162.58, 159.41, 152.79, 145.52, 145.37, 142.22, 133.03, 131.17, 128.58, 128.45, 127.79, 127.10, 124.51, 123.78, 119.26, 88.05, 40.85. ESI-MS *m/z*: 430.2 [M-H]⁻.

4.1.5.20 (Z)-*N*-(2-aminophenyl)-4-((2-(7-oxo-6,7-dihydro-5H-pyrrolo[3,4-*b*]pyridin-5-ylidene)acetamido)methyl)benzamide (**27b**). 40% isolated yield; white solid. Mp: 152-153 °C; ¹H NMR (300 MHz, DMSO-*d*₆) δ : 9.65 (s, 1H), 8.77 (s, 1H), 8.14 (d, *J* = 7.5 Hz, 1H), 7.93 (d, *J* = 7.2 Hz, 2H), 7.62-7.67 (m, 1H), 7.49 (d, *J* = 7.2 Hz, 2H), 7.15 (d, *J* = 5.6 Hz, 1H), 7.06-6.91 (m, 1H), 6.77 (d, *J* = 7.6 Hz, 1H), 6.61 (s, 1H), 6.56 (s, 3H, -NH₂), 4.86 (d, *J* = 16.0 Hz, 1H), 4.60 (d, *J* = 18.1 Hz, 1H); ¹³C NMR (75 MHz, DMSO-*d*₆) δ : 165.61, 165.05, 162.98, 161.66, 159.81, 151.60, 149.13, 145.54, 143.56, 142.52, 133.45, 130.94, 129.70, 128.84, 128.19, 127.82, 127.52, 126.76, 119.72, 86.64, 41.39. ESI-MS *m/z*: 412.1 [M-H]⁻.

4.1.5.21 (Z)-*N*-(2-amino-4-fluorophenyl)-4-((2-(7-oxo-6,7-dihydro-5H-pyrrolo[3,4-*b*]pyridin-5-ylidene)acetamido)methyl)benzamide (**27c**). 38% isolated yield; white solid. Mp: 205-207 °C; ¹H NMR (300 MHz, DMSO-*d*₆) δ : 9.58 (s, 1H), 8.76 (dd, *J*₁ = 1.3 Hz, *J*₂ = 4.8 Hz, 1H), 8.13 (dd, *J*₁ = 1.4 Hz, *J*₂ = 7.7 Hz, 1H), 7.93 (d, *J* = 8.2 Hz, 2H), 7.65 (dd, *J*₁ = 4.8 Hz, *J*₂ = 7.7 Hz, 1H), 7.48 (d, *J* = 8.2 Hz, 2H), 7.10 (dd, *J*₁ = 6.5 Hz, *J*₂ = 8.6 Hz, 1H), 6.60 (s, 1H), 6.53 (dd, *J*₁ = 2.8 Hz, *J*₂ = 11.2 Hz, 1H), 6.35 (td, *J*₁ = 2.9 Hz, *J*₂ = 8.5 Hz, 1H), 5.22 (s, 2H), 4.86 (d, *J* = 16.2 Hz, 1H), 4.59 (d, *J* = 16.3 Hz, 1H); ¹³C NMR (75 MHz, DMSO-*d*₆) δ : 165.34, 164.81, 162.57, 151.41, 148.73, 145.51, 145.36, 143.15, 133.05, 130.53, 129.29, 128.57, 128.43, 127.78, 127.41, 127.12, 126.36, 119.31, 86.23, 40.98. ESI-MS *m/z*: 430.2 [M-H]⁻.

4.1.5.22 *N*-(2-amino-4-fluorophenyl)-4-cyanobenzamide (**18**). 72% isolated yield; white solid. ¹H NMR (300 MHz, DMSO-*d*₆) δ : 9.87 (s, 1H), 8.13 (d, *J* = 8.2 Hz, 2H), 8.00 (d, *J* = 8.2 Hz, 2H), 7.21-6.98 (m, 1H), 6.62-6.44 (m, 1H), 6.44-6.25 (m, 1H), 5.34 (s, 2H); ESI-MS *m/z*: 256.3 [M+Na]⁺.

4.1.6 General procedure for the reaction of esters and hydroxylamine to afford hydroxamic acids **6** and **13a-b**

KOH (28 g, 509 mmol) and NH₂OH (23.35 g, 343 mmol) were dissolved in methanol (70 mL). After filtering the precipitate (KCl), a mix solution of NH₂OK and NH₂OH was obtained. Various esters (1 mmol) was dissolved in 10 mL NH₂OK solution and stirred overnight. After the reaction was complete, it was evaporated under vacuum. The residue was acidified with 1 N HCl to a pH 3-4 and then extracted with EtOAc (3 × 20 mL). The organic layer was washed with brine (2 × 30 mL) and dried over Na₂SO₄ overnight. The crude material was purified via flash chromatography to afford the product.

4.1.6.1 (Z)-*N*-hydroxy-4-((2-(3-oxoisindolin-1-ylidene)acetamido)methyl)benzamide (**6**). 72% isolated yield; white solid. Mp: 133-135 °C; ¹H NMR (300 MHz, DMSO-*d*₆) δ : 12.92 (s, 1H), 10.42 (s, 1H), 8.94 (t, *J* = 5.9 Hz, 1H), 7.92 (d, *J* = 8.2 Hz, 2H), 7.89-7.73 (m, 3H), 7.70-7.66 (m, 1H), 7.42 (d, *J* = 8.2 Hz, 2H), 6.10 (s, 1H), 4.49 (d, *J* = 5.8 Hz, 2H); ¹³C NMR (75 MHz, DMSO-*d*₆) δ : 167.78, 167.63, 166.75, 144.86, 143.64, 136.97, 133.48, 131.74, 129.94, 129.88, 129.38, 127.81, 123.79, 121.51, 95.64, 42.42. ESI-MS *m/z*: 360.2 [M+Na]⁺.

4.1.6.2 (Z)-*N*-hydroxy-6-(2-(3-oxoisindolin-1-ylidene)acetamido)hexanamide (**13a**). 71% isolated yield; white solid. Mp: 96-98 °C; ¹H NMR (300 MHz, DMSO-*d*₆) δ : 12.00 (s, 1H), 10.42 (s, 1H), 8.33 (t, *J* = 5.3 Hz, 1H), 7.94 – 7.55 (m, 4H), 6.01 (s, 1H), 3.19 (dd, *J*₁ = 7.0 Hz, *J*₂ = 12.1 Hz, 2H), 2.22 (t, *J* = 7.3 Hz, 2H), 1.50 – 1.53 (m, 4H), 1.38 – 1.27 (m, 2H). ¹³C NMR (75 MHz, DMSO-*d*₆) δ : 174.91, 167.71, 166.53, 143.02, 136.96, 133.41, 131.56, 129.36, 123.75, 121.39, 96.17, 38.90, 34.07, 29.27, 26.50, 24.69. ESI-MS *m/z*: 318.4 [M+Na]⁺.

4.1.6.3 (Z)-N-hydroxy-7-(2-(3-oxoisindolin-1-ylidene)acetamido)heptanamide (13b). 83% isolated yield; white solid. Mp: 164-165 °C; ¹H NMR (300 MHz, DMSO-*d*₆) δ: 12.03 (s, 1H), 10.42 (s, 1H), 8.36 (t, *J* = 5.5 Hz, 1H), 7.84-7.73 (m, 3H), 7.67 (m, 1H), 6.01 (s, 1H), 3.21-3.14 (m, 2H), 2.20 (t, *J* = 7.3 Hz, 2H), 1.58-1.35 (m, 4H), 1.29 (s, 4H); ¹³C NMR (75 MHz, DMSO-*d*₆) δ: 174.99, 167.67, 166.54, 143.01, 137.01, 133.41, 131.60, 129.41, 123.75, 121.40, 96.15, 39.00, 34.14, 29.38, 28.75, 26.68, 24.94. ESI-MS *m/z*: 354.1 [M+Na]⁺.

4.1.6.4 (Z)-N-(2-amino-5-fluorophenyl)-4-((2-(3-oxoisindolin-1-ylidene)acetamido)methyl)benzamide (5e).

To a solution of trifluoroacetic acid and CH₂Cl₂ (24 mL, v/v = 1:1) was added compound **9** (53.1mg, 0.1mmol). The mixture was stirred for 10 h at 0 °C. The reaction was quenched with Na₂CO₃ and the aqueous layer extracted with DCM (3×10 mL). The combined organic extracts were washed with brine, dried over sodium sulfate, concentrated in vacuo, and purified via flash chromatography, affording the product as a waxy solid. 61% isolated yield; Mp: 212-214 °C; ¹H NMR (300 MHz, DMSO-*d*₆) δ: 10.41 (s, 1H), 9.62 (s, 1H), 8.91 (t, *J* = 6.2 Hz, 1H), 7.95 (d, *J* = 8.2 Hz, 2H), 7.89-7.71 (m, 3H), 7.73-7.63 (m, 1H), 7.45 (d, *J* = 8.1 Hz, 2H), 7.23-7.11 (m, 1H), 6.89-6.73 (m, 2H), 6.11 (s, 2H), 4.83 (s, 2H), 4.50 (d, *J* = 6.0 Hz, 2H); ¹³C NMR (75 MHz, DMSO-*d*₆) δ: 167.24, 166.26, 165.15, 143.15, 142.95, 138.83, 136.48, 133.03, 132.97, 131.23, 128.90, 127.91, 127.10, 123.28, 121.00, 116.56, 112.57, 112.38, 112.29, 112.06, 95.14, 41.93. ESI-MS *m/z*: 453.1 [M+Na]⁺.

4.1.7 N-(2-amino-4-fluorophenyl)-4-(aminomethyl)benzamide (19)

To a solution of compound **18** (255.3 mg, 1 mmol) in methanol (10 mL) was added Pd/C (21.3 mg, 0.2 mmol). The mixture was heated to reflux for 5 h. After maximum conversion observed by TLC, the reaction mixture cooling to ambient temperature, the stock liquid was collected by filtration. Then the reaction mixture was diluted with 1 N HCl (0.5 mL). When the crystallizing was finished, the precipitate was collected as crude product by filtration. 61% isolated yield; white solid. Mp: 135-137 °C. ¹H NMR (300 MHz, DMSO-*d*₆) δ: 9.87 (s, 1H), 8.91 (s, 2H), 8.10 (d, *J* = 8.2 Hz, 2H), 7.99 (d, *J* = 8.2 Hz, 2H), 7.16-6.92 (m, 1H), 6.60-6.42 (m, 1H), 6.41-6.23 (m, 1H), 5.34 (s, 2H), 4.52 (s, 2H); ESI-MS *m/z*: 260.3 [M+Na]⁺.

4.1.8 6-hydroxy-5H-pyrrolo[3,4-*b*]pyridine-5,7(6H)-dione (22)

To a solution of furo[3,4-*b*]pyridine-5,7-dione (5 g, 33.56 mmol) in acetic acid (100 mL) was added hydroxylamine hydrochloride (2.80 g, 40.27 mmol). The reaction mixture was heated to reflux for 4 h. After maximum conversion observed by TLC, the reaction mixture was cooled to ambient temperature, concentrated in vacuo, then poured into water (40 mL), the formed precipitate was collected by filtration, washed with water, and dried in vacuo. 34% isolated yield; white solid. Mp: 163-165 °C. ¹H NMR (300 MHz, DMSO-*d*₆) δ: 11.03 (s, 1H), 8.95 (dd, *J*₁ = 1.4 Hz, *J*₂ = 5.0 Hz, 1H), 8.25 (dd, *J*₁ = 1.4 Hz, *J*₂ = 7.6 Hz, 1H), 7.79-7.75 (m, 1H); ESI-MS *m/z*: 163.0 [M-H]⁻.

4.2 In vitro HDAC enzyme assay

Enzyme inhibition activity were conducted by the Reaction Biology Corporation, Malvern, PA using HDAC fluorescent activity assay based on the unique Fluor de Lys™ substrate and developer combination. Compounds were dissolved in DMSO and tested in at least 10-dose IC₅₀ mode with 3-fold serial dilution starting at 50 μM. GraphPad Prism 5.0 software was used to calculate the IC₅₀ values for each compound.

4.3 In vitro cell growth inhibitory activity.

Culture medium and culture condition of cell lines. Cell growth inhibitory assay was conducted by 3D BioOptima, Co., Ltd. 1338 Wuzhong Blvd., Suzhou 215104, China using the Alamar blue cell growth inhibition

test module. HCT116 and MCF-7 human cancer cells were cultured in McCoy's 5A medium with 10% FBS, 100 U/mL penicillin and 100 ug/mL streptomycin. HL-60 cell was cultured in IMDM medium with 20% FBS, 100 U/mL penicillin and 100 ug/mL streptomycin. K562 was cultured in IMDM medium with 10% FBS, 100 U/mL penicillin and 100 ug/mL streptomycin. All cells were maintained at 37 °C in a humidified atmosphere of 5% CO₂ in air.

Cell Growth Inhibitory Assay. The general procedure using Alamar blue reagent for antiproliferative activities was as follows: 1. plated 100 µL cell suspension or completed medium into 96-well plate using a Matrix 12-channel pipettor. And filled residual wells with 200 µL PBS per well; 2. drugs were added to each well of 96-well plate; 3. placed plate into an incubator with corresponding culture condition for 72 h; 4. pipetted 22 µL Alamar blue solution (1 mM) into each well of 96-well plate; 5. returned plate to incubator and leave for 5~6 h; 6. shook plate for 10 seconds and recorded fluorescence at 530/590 nm.

4.4 Western Blotting

MCF-7 cells (1×10^6) were seeded overnight and then incubated with indicated concentrations of compounds for 24 h. Cell extract was prepared by lysing cultured cells with a mammalian protein extraction reagent supplemented with EDTA-free protease inhibitor for 15 min. Supernatants were collected following centrifugation of lysed cells at 15000 g for 10 min at 4 °C. To analyze the cell lysate, 30 µg of total protein per sample was resolved by SDS-PAGE and transferred onto a nitrocellulose membrane. Membranes with immobilized proteins were probed with antibodies for H3 acetylation. The reactive protein bands were visualized using an ECL detection system.

4.5 Growth Percent on 60 Cell Lines by NCI.

All detailed test method is described on the NCI Web site (https://dtp.cancer.gov/discovery_development/nci-60/methodology.htm).

4.6 Computational Methods

All computational work was performed in Discovery Studio 3.0 software (BIOVIA, 5005 Wateridge Vista Drive, San Diego, CA92121 USA). Docking was conducted using Cdocker module based on the cocrystal of HDAC1 (PDB: 5ICN). HDAC1 was used as the receptor. The cavity occupied by a peptide inhibitor was selected as binding site. The default values of docking sphere radius based on the peptide inhibitor was kept. Water molecules outside the binding pocket were excluded. The energy minimization for compounds was performed by Powell's method for 1000 iterations using tripos force field and with Gasteiger-Hückel charge. The other docking parameters were kept as default.

4.7 Microsomal stability assay

Each incubated mixture contained 0.5 mg/mL liver microsome (human or dog or rat), 100 mM potassium phosphate buffer (pH 7.4), 1 mM NADPH, and 1 µM test compound in a total volume of 200 µL. After prewarming at 37 °C for 10 min, the NADPH was added to initiate the reaction. The reaction was terminated after 0, 5, 10, 20, 40, or 60 min by adding 0.2 mg/mL glibenclamide (internal standard) in ice-cold methanol into 200 µL of incubation mixture. The sample was then centrifuged at 4000 rpm for 10 min at 4 °C. The supernatant was then analyzed by LC-MS/MS.

4.8 Pharmacokinetic analysis

All animal experiments were carried out in accordance with the U.K. Animals Act (1986) and associated

guidelines. The evaluation of compound was carried out using two separate sets of three male SD rats (199-214 g) after single iv (1 mg/kg) and po (10 mg/kg) administration. The animal was restrained manually at the designated time points, approximately 200 μ L of blood sample was collected via jugular vein into dried heparinized (coated with 0.25 % heparin in saline) tubes. Blood samples were centrifuged at 5500 rpm for 10 min to obtain plasma samples. An aliquot of 30 μ L of sample was added with 150 μ L CH_3CN which contains of Verapamil, 5 $\text{ng}\cdot\text{mL}^{-1}$ and Glibenclamide, 50 $\text{ng}\cdot\text{mL}^{-1}$ for protein precipitation. The mixture was vortexed for 10 min, and then centrifuged at 3700 rpm for 18 min. After that, 70 μ L of supernatant was added with 70 μ L of water, then vortexed for 10 min. An aliquot of 10 μ L of the mixture was injected into the LC-MS/MS system.

Acknowledgment

We thank the NCI Division of Cancer Treatment & Diagnosis for the NCI-60 screening of our compounds. This work was supported by Chinese Universities Scientific Fund (grant No. 2452017174), the Scientific Startup Foundation for Doctors of Northwest A&F University (grant No. 2452016146) and Natural Science Foundation of Jiangsu Province (grant No. BK20180573), China.

Appendix A. Supplementary data

Supplementary data related to this article can be found at

References

- [1] Minucci, S.; Pelicci, P. G., Histone deacetylase inhibitors and the promise of epigenetic (and more) treatments for cancer, *Nat. Rev. Cancer* 6 (1) (2006), 38-51.
- [2] Falkenberg, K. J.; Johnstone, R. W., Histone deacetylases and their inhibitors in cancer, neurological diseases and immune disorders, *Nat. Rev. Drug Discov.* 13 (9) (2014), 673-91.
- [3] Weichert, W., HDAC expression and clinical prognosis in human malignancies, *Cancer Lett.* 280 (2) (2009), 168-76.
- [4] Khan, O.; La Thangue, N. B., HDAC inhibitors in cancer biology: emerging mechanisms and clinical applications, *Immunol. Cell Biol.* 90 (1) (2012), 85-94.
- [5] Gammoh, N.; Lam, D.; Puente, C.; Ganley, I.; Marks, P. A.; Jiang, X., Role of autophagy in histone deacetylase inhibitor-induced apoptotic and nonapoptotic cell death, *Proc. Natl. Acad. Sci. USA* 109 (17) (2012), 6561-5.
- [6] De Ruijter, A. J.; van Gennip, A. H.; Caron, H. N.; Kemp, S.; van Kuilenburg, A. B., Histone deacetylases (HDACs): characterization of the classical HDAC family, *Biochem. J.* 370 (2003), 737-49.
- [7] Gregoret, I. V.; Lee, Y. M.; Goodson, H. V., Molecular evolution of the histone deacetylase family: functional implications of phylogenetic analysis, *J. Mol. Biol.* 338 (1) (2004), 17-31.
- [8] Kalin, J. H.; Bergman, J. A., Development and therapeutic implications of selective histone deacetylase 6 inhibitors, *J. Med. Chem.* 56 (16) (2013), 6297-313.
- [9] Weichert, W.; Roske, A.; Gekeler, V.; Beckers, T.; Stephan, C.; Jung, K.; Fritzsche, F. R.; Niesporek, S.; Denkert, C.; Dietel, M.; Kristiansen, G., Histone deacetylases 1, 2 and 3 are highly expressed in prostate cancer and HDAC2 expression is associated with shorter PSA relapse time after radical prostatectomy, *Br. J. Cancer* 98 (3) (2008), 604-10.
- [10] Weichert, W.; Roske, A.; Niesporek, S.; Noske, A.; Buckendahl, A. C.; Dietel, M.; Gekeler, V.; Boehm, M.; Beckers, T.; Denkert, C., Class I histone deacetylase expression has independent prognostic impact in human colorectal cancer: specific role of class I histone deacetylases in vitro and in vivo, *Clin. Cancer Res.* 14 (6) (2008), 1669-77.
- [11] Rikimaru, T.; Taketomi, A.; Yamashita, Y.; Shirabe, K.; Hamatsu, T.; Shimada, M.; Maehara, Y., Clinical significance of histone deacetylase 1 expression in patients with hepatocellular carcinoma, *Oncology* 72 (1-2) (2007), 69-74.
- [12] Miyake, K.; Yoshizumi, T.; Imura, S.; Sugimoto, K.; Batmunkh, E.; Kanemura, H.; Morine, Y.; Shimada, M., Expression of hypoxia-inducible factor-1 α , histone deacetylase 1, and metastasis-associated protein 1 in pancreatic carcinoma: correlation with poor

prognosis with possible regulation, *Pancreas*. 36 (3) (2008), e1-9.

[13] Marks, P. A.; Breslow, R., Dimethyl sulfoxide to vorinostat: development of this histone deacetylase inhibitor as an anticancer drug, *Nat. Biotechnol* 25 (1) (2007), 84-90.

[14] Sawas, A.; Radeski, D.; O'Connor, O. A., Belinostat in patients with refractory or relapsed peripheral T-cell lymphoma: a perspective review, *Ther. Adv. Hematol* 6 (4) (2015), 202-8.

[15] Laubach, J. P.; Moreau, P.; San-Miguel, J. F.; Richardson, P. G., Panobinostat for the Treatment of Multiple Myeloma, *Clin. Cancer Res.* 21 (21) (2015), 4767-73.

[16] Reddy, S. A., Romidepsin for the treatment of relapsed/refractory cutaneous T-cell lymphoma (mycosis fungoides/Sezary syndrome): Use in a community setting, *Crit. Rev. Oncol Hematol* 106 (2016), 99-107.

[17] Dong, M.; Ning, Z. Q.; Xing, P. Y.; Xu, J. L.; Cao, H. X.; Dou, G. F.; Meng, Z. Y.; Shi, Y. K.; Lu, X. P.; Feng, F. Y., Phase I study of chidamide (CS055/HBI-8000), a new histone deacetylase inhibitor, in patients with advanced solid tumors and lymphomas, *Cancer Chemother. Pharmacol.* 69 (6) (2012), 1413-22.

[18] Ning, Z. Q.; Li, Z. B.; Newman, M. J.; Shan, S.; Wang, X. H.; Pan, D. S.; Zhang, J.; Dong, M.; Du, X.; Lu, X. P., Chidamide (CS055/HBI-8000): a new histone deacetylase inhibitor of the benzamide class with antitumor activity and the ability to enhance immune cell-mediated tumor cell cytotoxicity, *Cancer Chemother. Pharmacol.* 69 (4) (2012), 901-9.

[19] Rekha Sangwan, Remya Rajan, Pintu Kumar Mandal, HDAC as onco target: Reviewing the synthetic approaches with SAR study of their inhibitors, *Eur. J. Med. Chem.* 158 (2018), 620-706.

[20] Chen Chen, Xuben Hou, Guohua Wang, Wenyan Pan, Xinying Yang, Yingkai Zhang, Hao Fang, Design, synthesis and biological evaluation of quinoline derivatives as HDAC class I inhibitors, *Eur. J. Med. Chem.* 133 (2017), 11-23.

[21] Rui Xie, Yue Yao, Pingwah Tang, Guangyao Chen, Xia Liu, Fan Yun, Chunhui Cheng, Xinying Wu, Qipeng Yuan, Design, synthesis and biological evaluation of novel hydroxamates and 2-aminobenzamides as potent histone deacetylase inhibitors and antitumor agents, *Eur. J. Med. Chem.* 134 (2017), 1-12.

[22] Yiwu Yao, Zhengchao Tu, Chenzhong Liao, Zhen Wang, Shang Li, Hequan Yao, Zheng Li, Sheng Jiang, *J. Med. Chem.* 58 (2015), 7672-7680.

[23] Luigi Aurelio, Celine Valant, Bernard L. Flynn, Patrick M. Sexton, Jonathan M. White, Arthur Christopoulos, Peter J. Scammells, Effects of Conformational Restriction of 2-Amino-3-benzoylthiophenes on A1 Adenosine Receptor Modulation, *J. Med. Chem.* 53(2010), 6550–6559.

[24] Kerry L. Spear, Monica S. Brown, Emily J. Reinhard, Ellen G. McMahon, Gillian M. Olins, Maria A. Palomo, Dennis R. Patton, Conformational Restriction of Angiotensin II: Cyclic Analogues Having High Potency, *J. Med. Chem.* 33 (1990), 1935-1940.

[25] Blasko, G.; Gula, D. J.; Shamma, M., The phthalideisoquinoline alkaloids, *J. Nat. Prod.* 45 (1982), 105–122.

[26] Valencia, E.; Fajardo, V.; Freyer, A. J.; Shamma, M., Magallanesine: an isoindolobenzazocine alkaloid, *Tetrahedron Lett.* 26 (1985), 993–996.

[27] Kato, Y.; Takemoto, M.; Achiwa, K., Synthesis and inhibitory activity of isoindolinone derivatives on thromboxane A2 ANALOG (U-46619)-induced vasocontraction, *Chem. Pharm. Bull.* 41 (1993), 2003–2006.

[28] Xin Chen, Feifei Ge, Tao Lu, Qingfa Zhou Stereoselective synthesis of 3-methyleneisoindolin-1-ones via base-catalyzed intermolecular reactions of electron-deficient alkynes with *N*-hydroxyphthalimides, *J. Org. Chem.* 80 (2015), 3295–3301.

[29] Mallu Chenna Reddy, Masilamani Jeganmohan, Ruthenium-catalyzed cyclization of aromatic nitriles with alkenes: stereoselective synthesis of (Z)-3-methyleneisoindolin-1-ones, *Org. Lett.* 16 (2014), 4866–4869.

[30] Shen S., Kozikowski A. P., Why hydroxamates may not be the best histone deacetylase inhibitors—what some may have forgotten or would rather forget? *ChemMedChem* 11 (2016), 15–21.

HIGHLIGHTS

- Potent class I HDAC inhibitors based on the natural isoindolinone scaffolds.
- Two azaisoindolinone scaffolds were first synthesized and characterized by X-ray crystallography.
- Molecular docking simulations suggested the key protein-ligand interactions for structural optimization.